



British  
Geological  
Survey



Environment  
Agency

# Analysis of climate variability and change in observational groundwater quality data

Environmental Change, Adaptation and Resilience Programme  
Commissioned Report CR/23/017



BRITISH GEOLOGICAL SURVEY

ENVIRONMENTAL CHANGE, ADAPTATION AND RESILIENCE  
PROGRAMME

COMMISSIONED REPORT CR/23/017

The National Grid and other  
Ordnance Survey data  
© Crown Copyright and  
database rights 2023.  
Ordnance Survey Licence  
No. 100021290 EUL.

*Bibliographical reference*

ASCOTT, M, GOODDY, D,  
MULCAHY, A, 2023.  
Analysis of climate variability  
and change in observational  
groundwater quality data.  
*British Geological Survey  
Commissioned Report,  
CR/23/017. 43pp.*

Copyright in materials derived  
from the British Geological  
Survey's work is owned by  
UK Research and Innovation  
(UKRI) and/or the authority  
that commissioned the work.  
You may not copy or adapt  
this publication without first  
obtaining permission. Contact  
the BGS Intellectual Property  
Rights Section, British  
Geological Survey, Keyworth,  
email [ipr@bgs.ac.uk](mailto:ipr@bgs.ac.uk). You  
may quote extracts of a  
reasonable length without  
prior permission, provided a  
full acknowledgement is given  
of the source of the extract.

Maps and diagrams in this  
book use topography based  
on Ordnance Survey  
mapping.

# Analysis of climate variability and change in observational groundwater quality data

M Ascott, D Goody, A Mulcahy

## BRITISH GEOLOGICAL SURVEY

Our range of publications is available from BGS shops at Nottingham, London and Cardiff (Welsh publications only). Shop online at [shop.bgs.ac.uk](http://shop.bgs.ac.uk).

We publish an annual catalogue of our maps and other publications; this catalogue is available online or from BGS shops.

*The British Geological Survey carries out the geological survey of Great Britain and Northern Ireland (the latter as an agency service for the government of Northern Ireland), and of the surrounding continental shelf, as well as basic research projects. It also undertakes programmes of technical assistance in geology in low- to middle-income countries.*

*The British Geological Survey is a component body of UK Research and Innovation.*

*British Geological Survey offices*

**Nicker Hill, Keyworth,  
Nottingham NG12 5GG**

Tel 0115 936 3100

**BGS Central Enquiries Desk**

Tel 0115 936 3143

email [enquiries@bgs.ac.uk](mailto:enquiries@bgs.ac.uk)

**BGS Sales**

Tel 0115 936 3241

email [sales@bgs.ac.uk](mailto:sales@bgs.ac.uk)

**The Lyell Centre, Research Avenue South,  
Edinburgh EH14 4AP**

Tel 0131 667 1000

**Natural History Museum, Cromwell Road,  
London SW7 5BD**

Tel 020 7589 4090

Tel 020 7942 5344/45

email [bgs-londonstaff@bgs.ac.uk](mailto:bgs-londonstaff@bgs.ac.uk)

**Cardiff University, Main Building, Park Place,  
Cardiff CF10 3AT**

Tel 029 2167 4280

**Maclean Building, Crowmarsh Gifford,  
Wallingford OX10 8BB**

Tel 01491 838800

**Geological Survey of Northern Ireland, Department for  
the Economy, Dundonald House, Upper Newtownards  
Road, Ballymiscaw, Belfast, BT4 3SB**

Tel 0289 038 8462

[www2.bgs.ac.uk/gsni/](http://www2.bgs.ac.uk/gsni/)

**Natural Environment Research Council, Polaris House,  
North Star Avenue, Swindon SN2 1EU**

Tel 01793 411500

Fax 01793 411501

[www.nerc.ac.uk](http://www.nerc.ac.uk)

**UK Research and Innovation, Polaris House,  
Swindon SN2 1FL**

Tel 01793 444000

[www.ukri.org](http://www.ukri.org)

Website [www.bgs.ac.uk](http://www.bgs.ac.uk)

Shop online at [shop.bgs.ac.uk](http://shop.bgs.ac.uk)

# Contents

Executive Summary .....	iv
1 Introduction.....	1
2 Co-design of choice of determinands, methodology, research questions and implications ..	1
3 Nitrate analysis .....	2
3.1 Methodology.....	2
3.2 Results .....	5
3.3 Discussion.....	17
3.4 Conclusions.....	20
4 Groundwater temperature analysis.....	21
4.1 Methodology.....	21
4.2 Results .....	24
4.3 Discussion.....	31
4.4 Conclusions.....	34
References.....	34

## FIGURES

Figure 1 Location of nitrate time series from subset 2 and observation boreholes. WIMS data © Environment Agency copyright and/or database right 2023. ....	5
Figure 2 Locations of sampling points (red) meeting the different screening criteria overlain on EA areas. WIMS data © Environment Agency copyright and/or database right 2023. EA areas © Environment Agency and/or database right 2016. All rights reserved. ....	7
Figure 3 Locations of sampling points (red) meeting the different screening criteria overlain on simplified 1:625,000 scale hydrogeological maps. WIMS data © Environment Agency copyright and/or database right 2023. ....	8
Figure 4 Number of sampling points per EA area for each subset (top to bottom). Criteria for each subset are shown in Table 2.....	9
Figure 5 “Missingness” plot for all data from subset 2 (1989-2022). Each column represents a site, and each row (observation) is a month. Columns (sites) are ordered from left to right from least to most complete. The red lines indicate the time period sub-sampled for the cluster analysis (1995-2020, shown in full in Figure 6). ....	10
Figure 6 “Missingness” plot for data from subset 2 used in the cluster analysis (1995-2020), corresponding to area between the red lines in Figure 5. ....	10
Figure 7 K means “elbow” plot to determine the most appropriate number of clusters.....	11
Figure 8 Heatmap and dendrogram for standardised nitrate time series in subset 2. Red and blue colours indicate higher and lower concentrations respectively. Uses WIMS data © Environment Agency copyright and/or database right 2023. ....	12
Figure 9 Normalised nitrate time series for cluster centroids with k=4. Uses WIMS data © Environment Agency copyright and/or database right 2023. ....	13
Figure 10 Spatial distribution of nitrate clusters overlain on EA areas. Uses WIMS data © Environment Agency copyright and/or database right 2023. EA areas © Environment Agency and/or database right 2016. All rights reserved. ....	14

Figure 11	Spatial distribution of nitrate clusters overlain on 1:625,000 scale hydrogeological map. Uses WIMS data © Environment Agency copyright and/or database right 2023.....	14
Figure 12	Boxplot of borehole depths for the different clusters.....	15
Figure 13	Maximum correlations and lags between standardised detrended monthly nitrate concentrations and monthly precipitation totals (left), monthly mean groundwater levels (centre), and standardised groundwater level index (SGI, right), split by cluster.....	16
Figure 14	Boxplots of correlation (left), accumulation period (middle), and lag (left) for Standardised Precipitation Index (SPI)-standardised detrended monthly nitrate concentration correlations.....	16
Figure 15	Standardised Precipitation Index (SPI) lags and accumulation periods for cluster 1 and 2 as a function of correlation coefficient $r$ .....	16
Figure 16	Simplified conceptual model of changes in nitrate fluctuations as a function of changing piston flow under climate change causing increased GWL fluctuation and varying unsaturated zone nitrate profiles.....	19
Figure 17	Location of groundwater, river and air temperature time series and 1:625,000 scale bedrock geology. Contains Ordnance Survey data © Crown copyright and database right 2023. Ordnance Survey Licence No. 100021290 EUL.....	22
Figure 18	Groundwater temperature time series for BGS and Affinity Water sites. Affinity Water data © Affinity Water.....	25
Figure 19	Groundwater temperature time series at PTM21 and air temperature time series at Oxford for 2003-2017 (left) and 1970-2020 (right). Air temperature data reproduced from Burt and Burt (2019).....	25
Figure 20	Groundwater temperature time series for BGS and Affinity Water sites. Each site is plotted on individual y-axis scales and PTM21 has been removed for clarity. Affinity Water data © Affinity Water.....	26
Figure 21	Seasonal cycle in groundwater temperature time series. Affinity Water data © Affinity Water.....	27
Figure 22	Diurnal cycle in groundwater temperature time series. Affinity Water data © Affinity Water.....	27
Figure 23	Groundwater temperature time series in the frequency domain.....	28
Figure 24	Diurnal cycle in groundwater temperature time series at Denge 24, Denge Middle and WL stratified by season. Affinity Water data © Affinity Water.....	29
Figure 25	Trends in groundwater, air and river temperature time series. Affinity Water data © Affinity Water.....	29
Figure 26	Correlations between time series metrics and metadata. Affinity Water data © Affinity Water.....	30

## TABLES

Table 1	Determinands, research questions, implications and summary of methodology for the determinands assessed in this task.....	1
Table 2	Screening criteria used to determine suitability of sites for assessment of impacts of climate variability on nitrate time series.....	3
Table 3	Number of sampling points for the different screening criteria.....	6
Table 4	Metadata for groundwater temperature time series. Interfluve boreholes are marked with an asterisk. Affinity Water data © Affinity Water.....	23

# Executive Summary

This report details Task 1 (“Evaluation of historical observational groundwater quality data”) of Phase 2 of the Environment Agency-BGS collaborative project “climate and land use change impacts on groundwater quality”. The objective of this task is to evaluate historical observational groundwater quality data held by the Environment Agency (EA) to determine the following: (1) the suitability of existing monitoring for future monitoring of long-term impacts of climate and land use change and (2) whether there is evidence for climate variability, and if possible, impacts of historical climate change in the observations. It was agreed in an EA-BGS kickoff meeting that this task would investigate climate variability and change in nitrate and groundwater temperature data. This task focusses on southeast England as a case study.

Analysis of groundwater nitrate data held by the Environment Agency in WIMS has shown that a small number of sites meet the required time series length requirement for climate change impact monitoring in southeast England (30 years). The recent natural variability in climate combined with short record length means that any climate change impacts cannot be observed in the data provided. Cluster analysis has revealed different modes of temporal fluctuations in nitrate concentrations. The depth of groundwater flow system intercepted by the boreholes appears to control the long-term direction of change in groundwater nitrate concentrations. Non-linear and seasonal behaviour associated with climate variability are present in two clusters, which are weakly spatially coherent across the North and South Downs. Cross-correlation of nitrate time series with both raw and standardised indices of groundwater level and precipitation show that the extent of nitrate fluctuation appears to be controlled by precipitation and groundwater level fluctuation. This may be due to a combination of piston flow and changing groundwater flow paths. Under future climate change, nitrate fluctuations may change associated with the changing intersection of the water table and the legacy nitrate peak in the unsaturated zone. The timescales for land use change impacts on nitrate at the water table will vary substantially depending on the dominant process controlling nitrate fluctuations. Processes which represent a transfer of mass (bypass flow) will impact concentrations much more rapidly than processes representing a transfer of energy (piston flow).

Analysis of groundwater temperature data for 20 boreholes has shown that, for 8 of 17 shallow boreholes with temperature data over 2012-2022, groundwater temperature trends are broadly consistent with current air temperature trends. 7 of these sites show increasing trends, with a mean trend of 0.66 °C/decade. Three deep interfluvial sites show increases, with a mean trend of 0.38 °C/decade. It is likely that these trends are controlled by current and historical near-decadal trends in local air temperature for shallow and deep sites respectively. The remaining 8 shallow sites show inconsistent trends in comparison with local air temperature trends. For these sites it is likely that in addition to air temperature trends, additional heat fluxes into the subsurface are occurring superimposed on changes in groundwater flow to the boreholes. The shallow sites show seasonal temperature fluctuations associated with propagation of air temperature signals, with seasonal range in groundwater temperature significantly negatively correlated with borehole depth. Three very shallow sites show diurnal fluctuations, although these fluctuations are below the accuracy of the sensors. The increases in groundwater temperature observed have some implications for other components of groundwater quality (e.g. biogeochemical cycles, stygofauna, pollutant (N, pesticide, LNAPL) degradation and for the role that groundwater discharges to surface water play in providing cold-water hydro-refugia to cold-water species during summer.

# 1 Introduction

This report presents the results of task 1 of phase 2 of the climate change and groundwater quality project. The objective of task 1 is to evaluate historical observational groundwater quality data held by the Environment Agency (EA) to determine the following: (1) the suitability of existing monitoring for future monitoring of long-term impacts of climate and land use change and (2) whether there is evidence for climate variability, and if possible, impacts of historical climate change in the observations. This task focusses on southeast England as a case study.

This report is structured as follows. Section 2 reports the outcomes of the task kick-off meeting in which the determinands, hypotheses to be tested and approach were co-designed with the EA project steering group. Sections 3 and 4 respectively report the detailed methodology, results, discussion and conclusions for analyses of nitrate and groundwater temperature data respectively.

## 2 Co-design of choice of determinands, methodology, research questions and implications

On 10<sup>th</sup> October 2022 a kick-off meeting for this task was held between BGS and the EA project steering group. This meeting was held to agree the determinands and approach for the analysis, and the research questions that the analysis would address and the likely implications of the work. Table 1 reports the results of the kick-off meeting.

Table 1 Determinands, research questions, implications and summary of methodology for the determinands assessed in this task

Determinand	Research questions	Implications	Methodology
Nitrate	Which boreholes are suitable long term monitoring points for climate and land use change impacts?	Where to prioritise future monitoring, conceptual models of how climate change may affect nitrate concentrations	Screening WIMS nitrate data, cluster analysis, cross-correlation analysis
	How does this vary across EA areas and aquifers?		
	Which boreholes show evidence of climate variability? What are the controls?		
	Is there any evidence for climate change?		



Determinand	Research questions	Implications	Methodology
Groundwater temperature	Is there evidence for groundwater temperatures increasing as a function of climate variability and change?	Increasing temperatures of groundwater discharge to ecologically sensitive groundwater dependent terrestrial ecosystems and high baseflow streams, changes to other groundwater quality variables through changing reaction rates, groundwater ecology, ground source heat pump feasibility, utility of existing datasets for GWT monitoring and sensors for future datasets	Collation of water company groundwater temperature data, time series analysis
	How do groundwater temperatures vary across different temporal and spatial scales?		

In the kick-off meeting it was also suggested that microbial contaminants (e.g. e. coli, total coliforms) could also be investigated. Data for these determinands were not able to be provided for this project and therefore are not considered further in this report.

## 3 Nitrate analysis

### 3.1 METHODOLOGY

#### 3.1.1 Datasets and preprocessing

An extract of the WIMS database was provided by the Environment Agency for nitrate and nitrite. The following criteria were used to extract WIMS data:

- Only dete codes corresponding to nitrate (as N (117), as NO<sub>3</sub> (9880) and nitrite (118))
- Only purpose codes: MN, MP, MS, MU, PN, XO
- Only SMPT\_type: BA, BB, BC, BD, BZ, GD, GF
- Only material: 2ZZZ, 2EZZ, 2EBZ
- Data from EA areas in southeast England only (Solent and South Downs, Hertfordshire and North London, West Thames, Kent and South London)

For full descriptions of the purpose codes, sampling point types and materials used, the reader is referred to the reference of the Environment Agency's Water Quality Archive (<https://environment.data.gov.uk/water-quality/view/doc/reference>). The resulting dataset contained 328,837 measurements covering all three of the dete codes above. Nitrite data were not considered in this analysis, which resulted in 219,699 measurements in total for nitrate (67% of the dataset) made up of nitrate as N (126,535 measurements) and nitrate as NO<sub>3</sub> (93,164 measurements).

The nitrate as NO<sub>3</sub> data were exclusively "EXTERNAL ORGANISATION MONITORING (NOT FOR PUBLICATION)" for EA Areas in the Thames and Southern regions. These data were converted to nitrate as N. Where this resulted in a single sample (as recorded by MEAS\_SAMPLE\_ID) having multiple nitrate as N measurements, the converted measurements was removed. This occurred for 7,003 measurements. Consequently 86,161 measurements were added to the 126,535 original nitrate as N samples to produce a final dataset with 212,696 nitrate as N measurements.

### 3.1.2 Screening sites suitable for assessment of impacts of climate variability on nitrate time series

For each unique sampling point (SMPT\_USER\_REFERENCE) we extracted the number of samples, the first and last year of samples, and the regularity index,  $R$ , defined by Stuart et al. (2007) as the ratio of the mean to the standard deviation of the gap between samples. Sampling points containing the strings “TREATED” (19 points) or “FINAL” (9 sample points) in SMPT\_LONG\_NAME were removed. These were external organisation sites (Water Companies) in the Solent and South Downs area.

Stuart et al. (2007) used a series of criteria (minimum 5 years of data, a minimum of 20 samples and  $R = 0.5$ ) to screen for trends in nitrate data. These criteria are highly lenient in the context of climate variability and change, with 30 years of data considered to be necessary to evaluate climate change impacts by the WMO (World Meteorological Organization, 2017). We therefore developed a bespoke set of different criteria building on the approach of Stuart et al. (2007) and WMO time series length guidelines. These are shown in Table 2. Four different filters were used, with the most stringent and lenient following WMO guidelines and Stuart et al. (2007) respectively. On testing the WMO guideline filter this resulted in only 19 sites, and so additional filters for 20 and 10 years of data were also included.

Table 2 Screening criteria used to determine suitability of sites for assessment of impacts of climate variability on nitrate time series

Subset number	Number of years	Number of samples	$R$	Justification
1	30	360	0.5	WMO recommended number of years, on average one sample per month, same regularity as Stuart et al. (2007)
2	20	240	0.5	20 years of data, on average one sample per month, same regularity as Stuart et al. (2007)
3	10	120	0.5	10 years of data, on average one sample per month, same regularity as Stuart et al. (2007)
4	5	20	0.5	Criteria used by Stuart et al. (2007)

We plotted and aggregated the results of the screening spatially with EA areas and aquifers. It was not possible to aggregate results by purpose codes as some monitoring points had multiple purpose codes that change over time. An example of this is water company abstractions, where for a unique SMPT\_USER\_REFERENCE there are multiple purpose codes that reflect both EA and water company monitoring of the same abstraction.

### 3.1.3 Cluster analysis to group modes of temporal variability in nitrate time series

Following a review of the sites for the different subsetting criteria in section 3.1.2, only subset 2 was considered to be an acceptable balance of the number of sites and amount of missing data. For subset 2 we then evaluated the different modes of temporal variability in the nitrate time series using a cluster analysis approach, as follows.

Measurements where concentrations were below the limit of detection were set to half of the limit of detection (0.196 mg N/L). In subset 2, 0.62% of the measurements across all the time series were below the limit of detection. For each time series we resampled nitrate concentration values to monthly means to avoid biases in the number of samples per unit time. We then plotted a “missingness” heatmap to evaluate the extent of missing data across all the time series. We used this heatmap to further sub-sample the data by

truncating the start and end of all the time series to 1995 to 2021 respectively, to ensure most sites had regular data. Data outside of this period was not considered further. An example of how choosing this period affects the data used in the cluster analysis is shown in Figure 5 and Figure 6.

We then standardised the data for each time series such that mean = 0 and standard deviation = 1. Missing values were imputed by linear interpolation. To determine the most appropriate number of clusters, we first undertook hierarchical clustering using Euclidean distance and the complete linkage method (Webster and Oliver, 1990) to produce an ordered heatmap and cluster dendrogram. We also undertook K means clustering for  $k = 1$  to 15 and estimated the within clusters sum of squares to produce the K means “elbow” plot. We visually inspected the resulting plots that showed a suitable number of clusters was  $k = 4$ .

We then repeated the k means cluster analysis with  $k = 4$ , using 10,000 random sets as starting centres. We plotted the time series of the cluster centres and mapped the cluster membership across England.

#### **3.1.4 Evaluation of controls on temporal variability between nitrate time series**

We evaluated 5 potential controls on temporal variability between nitrate time series principally associated with hydrogeological and hydroclimatic setting; borehole depth, monthly precipitation totals, the standardised precipitation index (SPI), monthly mean groundwater levels and the standardised groundwater level index (SGI). As SGI and SPI are standardised (i.e. mean = 0, standard deviation = 1), direct comparison between sites can be made. Both SGI and SPI are also deseasonalised so are potentially a better metric of anomalously high or low hydrometeorological status relative to seasonal norms. Finally, SPI is also calculated for a range of precipitation accumulation periods in months. Calculating SPI over longer accumulation periods results in a more “smoothed” signal. Assessment of what accumulation period SPI best correlates with SGI has been shown to be a powerful technique to evaluate controls on clustering of groundwater level time series (Ascott et al., 2017; Bloomfield et al., 2015), and we would anticipate the use of this approach to also be of benefit in understanding controls on clustering of groundwater nitrate time series.

For each of the sites in subset 2 we extracted the borehole depth from an extract of the EA’s Boreholes, Wells and Springs database provided for this project. We then produced a box plot to compare the borehole depths across the 4 clusters and used a one-way analysis of means (not assuming equal variances) to determine if there were significant differences between the clusters.

We extracted monthly precipitation totals for each site from the HadUK-Grid dataset (Hollis et al., 2019). Bilinear interpolation was used so that for each site, values were interpolated from the four nearest raster cells. We cross-correlated the detrended standardised monthly nitrate concentrations with the monthly precipitation totals for each site and recorded the maximum value of the Pearson’s correlation coefficient and the accompanying lag. We then plotted the lags and correlation coefficients as a function of cluster membership.

For the monthly precipitation totals extracted from HadUK-Grid, we then calculated SPI using accumulation periods from 1 to 48 months (McKee et al., 1993). For each site, we cross-correlated the detrended standardised monthly nitrate concentrations with SPI-1 to SPI-48. The maximum correlation between nitrate and SPI was recorded with the associated SPI accumulation period and lag. Boxplots and scatterplots were used to visualise differences between the clusters related to SPI-Nitrate correlations, SPI accumulation periods and SPI lags.

To correlate nitrate time series with groundwater level time series, each site had to be related to an observation borehole. Groundwater level time series for each sampled borehole were not available, and will be highly affected by abstraction in any case. Consequently, each site was linked to its nearest observation borehole used by BGS in

monthly hydrological outlooks and summaries (known as “index” boreholes). The locations of the nitrate time series and the observation boreholes are shown in Figure 1. These boreholes are known to have minimal influence from groundwater abstraction (Prudhomme et al., 2017) and therefore represent a reasonable proxy for regional groundwater level status across the Chalk and Oolitic limestone regions of Southern England. We extracted monthly mean groundwater level time series for each observation borehole, and cross correlated detrended standardised monthly nitrate concentrations with standardised groundwater levels (mean = 0, standard deviation 1, note this is not the same as the SGI), and recorded the maximum value of the Pearson’s correlation coefficient and the accompanying lag. We then plotted the lags and correlation coefficients as a function of cluster membership. The same methodology was then repeated for correlations between detrended standardised monthly nitrate concentrations with SGI (using 1995-2022 as a reference period).

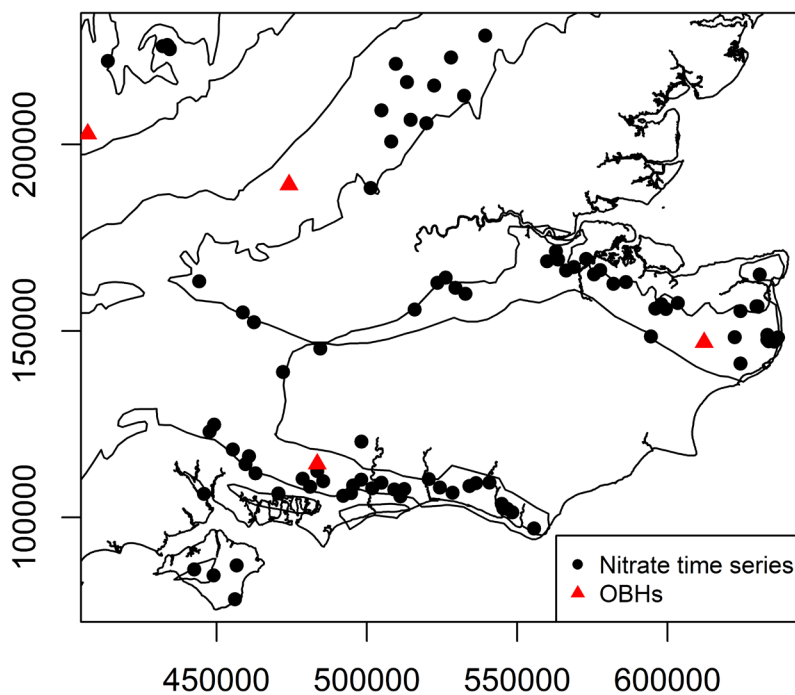


Figure 1 Location of nitrate time series from subset 2 and observation boreholes. WIMS data © Environment Agency copyright and/or database right 2023.

## 3.2 RESULTS

### 3.2.1 Suitability of sites for assessment of impacts of climate variability on nitrate time series

In total there were 1,948 unique sampling points in southeast England in the processed WIMS dataset provided. The total number of sampling points per subset is shown in Table 3. The locations of the points in comparison to EA areas and simplified 1:625,000 scale hydrogeological maps are shown in Figure 2 and Figure 3 respectively.

Figure 4 shows the breakdown of sampling points across EA areas in southeast England for the different subsets.

Applying the most stringent criteria (subset 1, 30 years of data based on WMO guidance) to the data provided resulted in only 19 sampling points. These are exclusively Chalk abstraction boreholes in the Solent and South Downs and Kent and South London areas, monitored by Southern Water and labelled “EXTERNAL ORGANISATION MONITORING”. Reducing the number of years to 20 (subset 2) increased the number of sampling points to 96. Similar to subset 1, the sampling points are almost entirely on the Chalk, with a small number of sites on the Cotswold Oolites and Lower and Upper Greensands. In subset 2 there is coverage of across all EA areas in southeast England.

Reducing the number of years further to 10 (subset 3) increased the number of sampling points to 244. The distribution of sampling points remains dominated by the Chalk, although there are several points off the Chalk outcrop including the Weald in Kent. Applying the least stringent criteria (subset 4, based on Stuart et al. (2007)) resulted in 919 sampling points. There is a much more widespread coverage of sampling points across southeast England.

Table 3 Number of sampling points for the different screening criteria

Subset number	Number of years	Number of samples	Regularity	Justification	Number of sampling points	% of total sampling points
1	30	360	0.5	WMO recommended number of years, on average one sample per month, same regularity as Stuart et al. (2007)	19	0.97
2	20	240	0.5	20 years of data, on average one sample per month, same regularity as Stuart et al. (2007)	96	4.98
3	10	120	0.5	10 years of data, on average one sample per month, same regularity as Stuart et al. (2007)	244	12.5
4	5	20	0.5	Criteria used by Stuart et al. (2007)	919	47.2

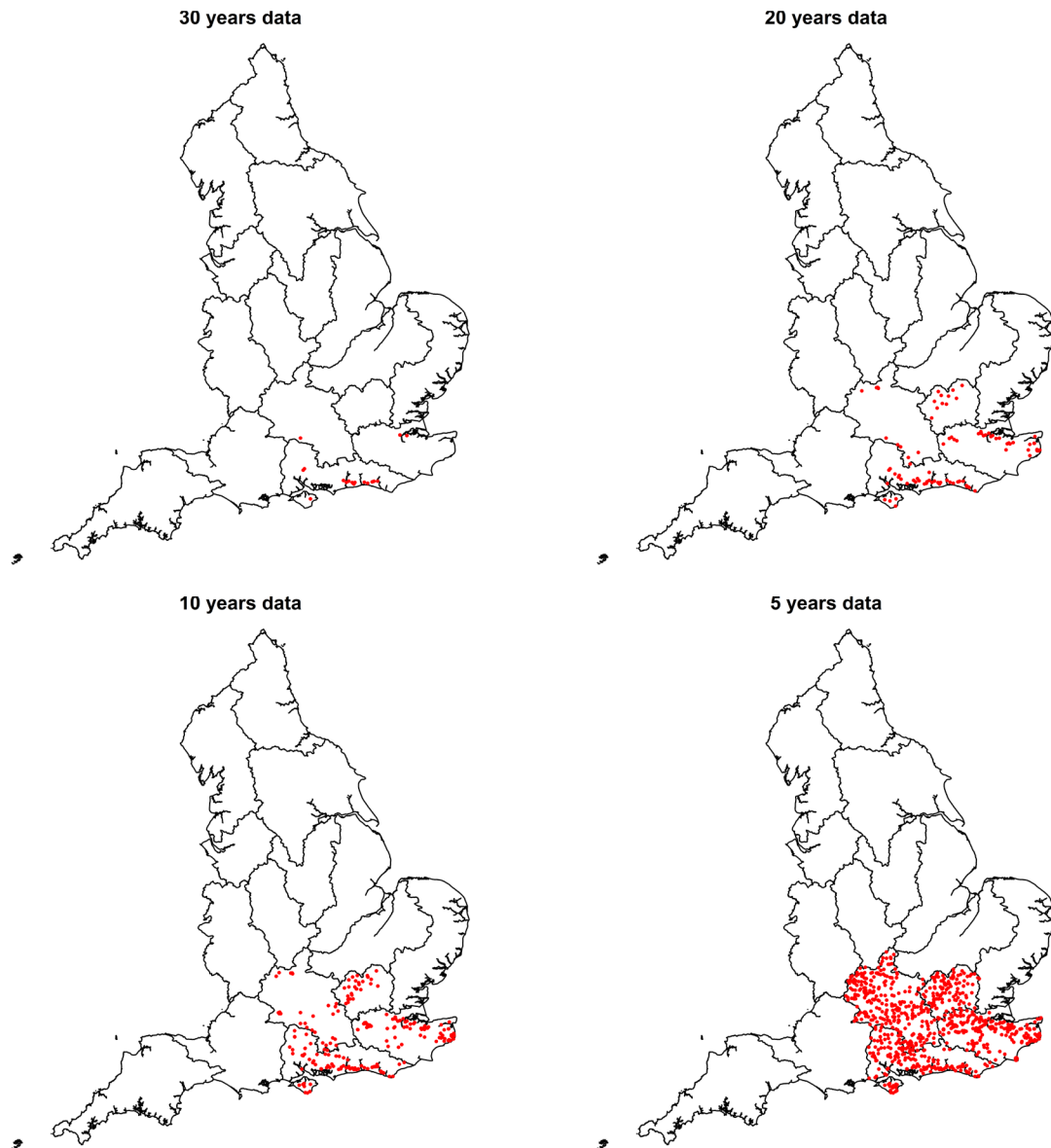


Figure 2 Locations of sampling points (red) meeting the different screening criteria overlain on EA areas. WIMS data © Environment Agency copyright and/or database right 2023. EA areas © Environment Agency and/or database right 2016. All rights reserved.



Figure 3 Locations of sampling points (red) meeting the different screening criteria overlain on simplified 1:625,000 scale hydrogeological maps. WIMS data © Environment Agency copyright and/or database right 2023.

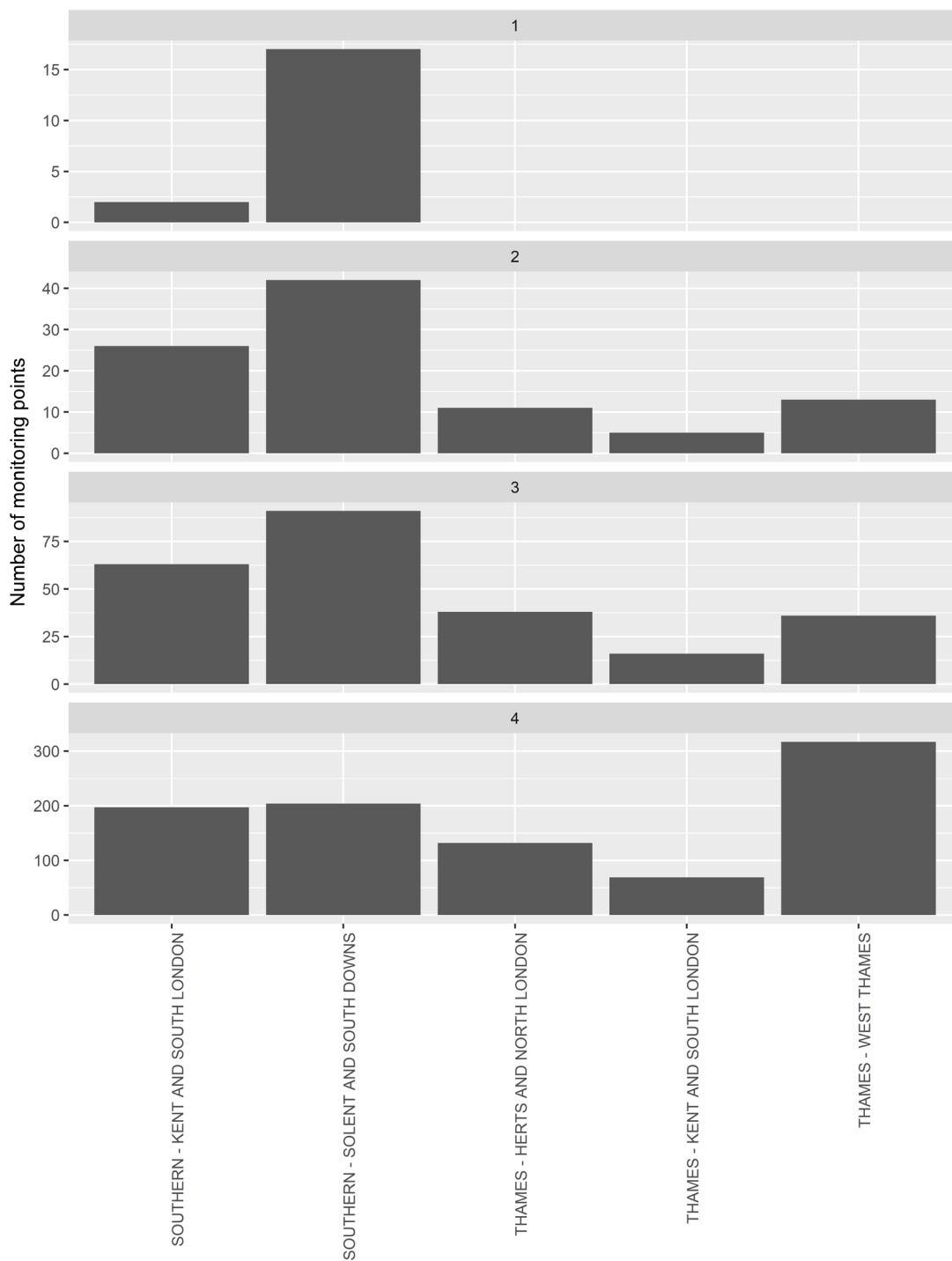


Figure 4 Number of sampling points per EA area for each subset (top to bottom). Criteria for each subset are shown in Table 2.



### 3.2.2 Cluster analysis

Figure 5 shows the extent of missing data from subset 2 when resampled to monthly mean values. There are significant gaps in the data particularly at the start (pre-1995/observation 80) and end (post-2020/observation 375) of the record.

Figure 6 shows the extent of the missing data when subset 2 is sub-sampled further to only include data from 1995 to 2020. This substantially reduces the amount of missing data, although there are still several sites with missing data in early years.

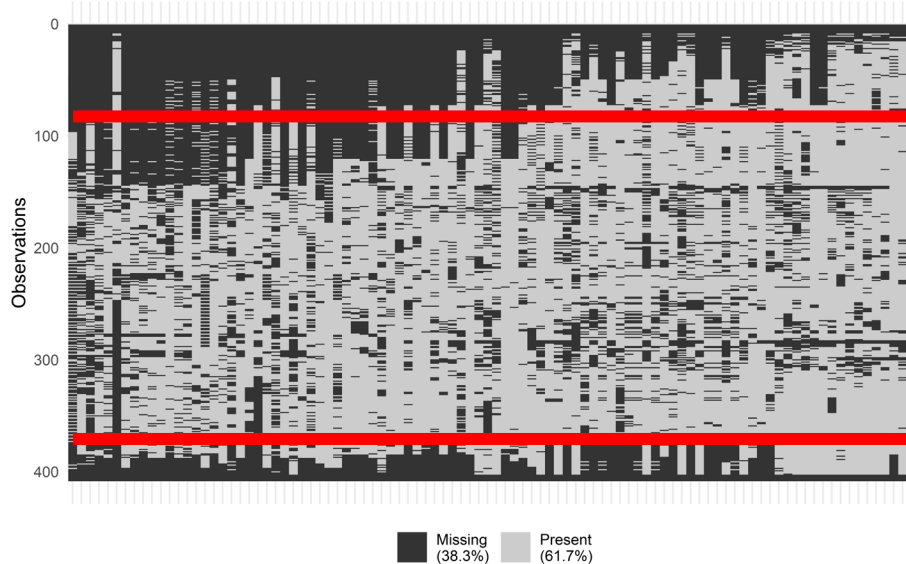


Figure 5 “Missingness” plot for all data from subset 2 (1989-2022). Each column represents a site, and each row (observation) is a month. Columns (sites) are ordered from left to right from least to most complete. The red lines indicate the time period sub-sampled for the cluster analysis (1995-2020, shown in full in Figure 6).

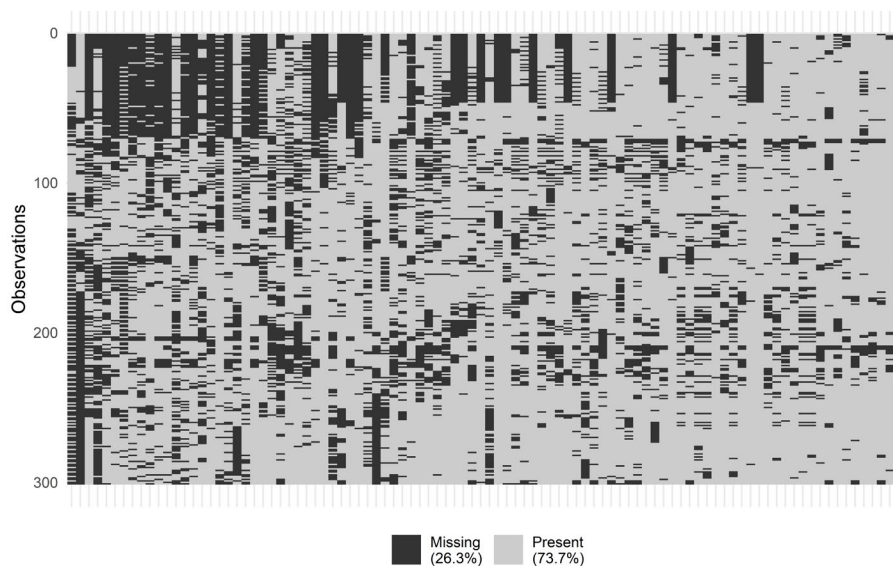


Figure 6 “Missingness” plot for data from subset 2 used in the cluster analysis (1995-2020), corresponding to area between the red lines in Figure 5.

Figure 7 shows the within groups sum of squares derived from undertaking k means clustering for k = 1 to 15. This shows the within groups sum of squares decreases substantially from k = 1 to 2. From k = 2 upwards, there is no clear break of slope.

Figure 8 shows the heatmap and dendrogram derived by hierarchical cluster analysis of the standardised nitrate time series in subset 2. A first order control on cluster partition (i.e. k = 2) appears to be whether sites show an overall increasing or decreasing trend over time. Broken down further, visually the time series can be grouped as follows: sites that show near-linear increases through time; sites that show near-linear decreases through time; sites with seasonal behaviour superimposed on a long-term increasing trend; and sites with non-linear behaviour superimposed on a long-term increasing trend. The same results are borne out when undertaking k-means cluster analysis for k = 4, as shown in the cluster centroid time series in Figure 9. For the rest of this analysis, the clusters will be referred to as follows based on Figure 9:

- Cluster 1 – non-linear behaviour and increasing trend
- Cluster 2 – seasonal behaviour and increasing trend
- Cluster 3 – near-linear increasing trend
- Cluster 4 – near-linear decreasing trend

Figure 10 and Figure 11 show the spatial distribution of the cluster membership in comparison to EA areas and the 1:625,000 scale hydrogeological map respectively. There is no strong spatial coherence to the cluster membership, although visually it appears that cluster 2 may be predominantly in the South Downs and cluster 1 in the North Downs. Of all the sites in cluster 2, 75% are with the South Downs. Of all the sites in cluster 1, 57% are in the North Downs.

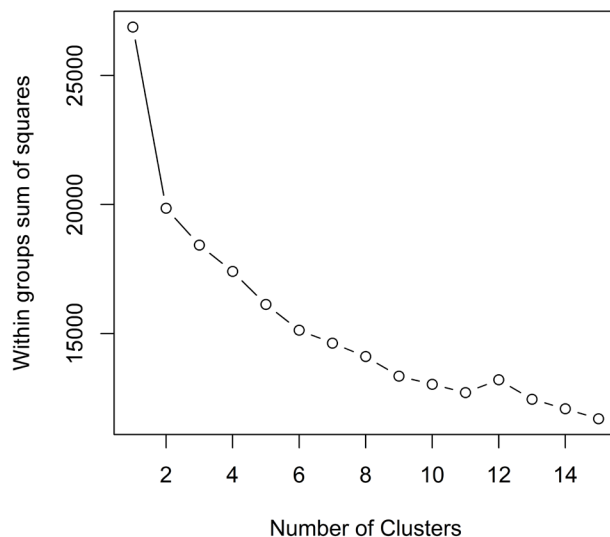


Figure 7 K means “elbow” plot to determine the most appropriate number of clusters

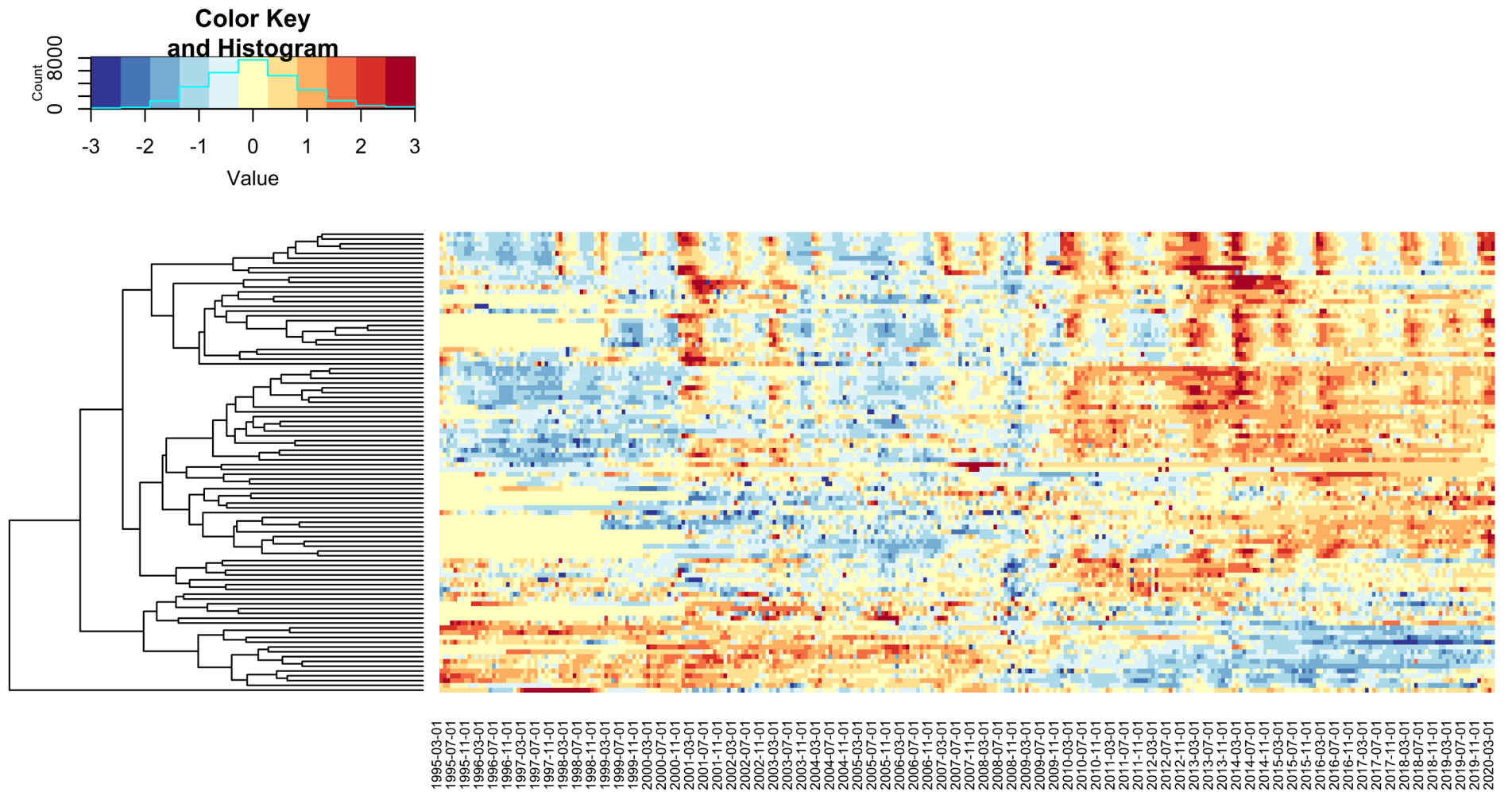


Figure 8 Heatmap and dendrogram for standardised nitrate time series in subset 2. Red and blue colours indicate higher and lower concentrations respectively. Uses WIMS data © Environment Agency copyright and/or database right 2023.

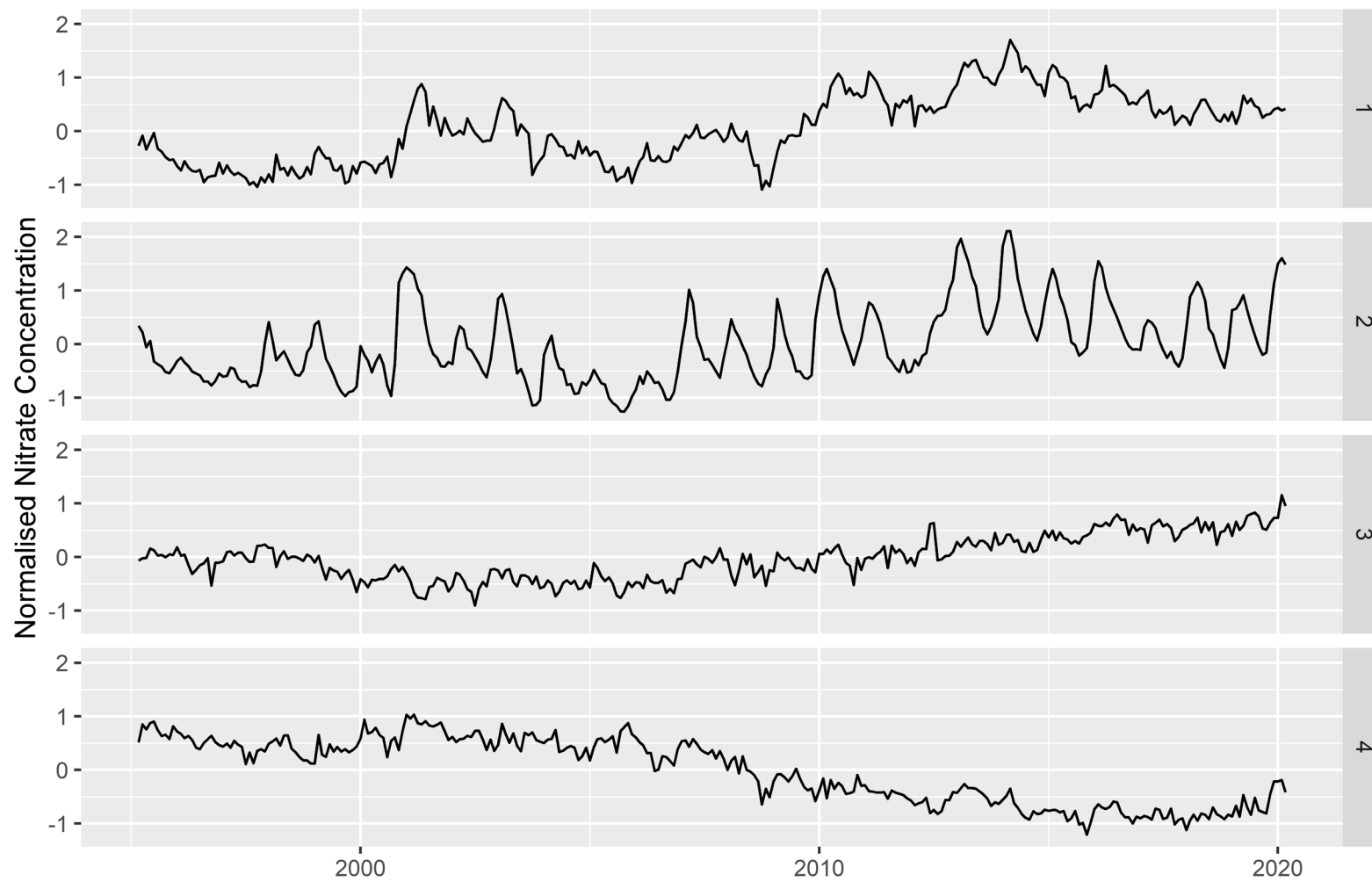


Figure 9 Normalised nitrate time series for cluster centroids with  $k=4$ . Uses WIMS data © Environment Agency copyright and/or database right 2023.

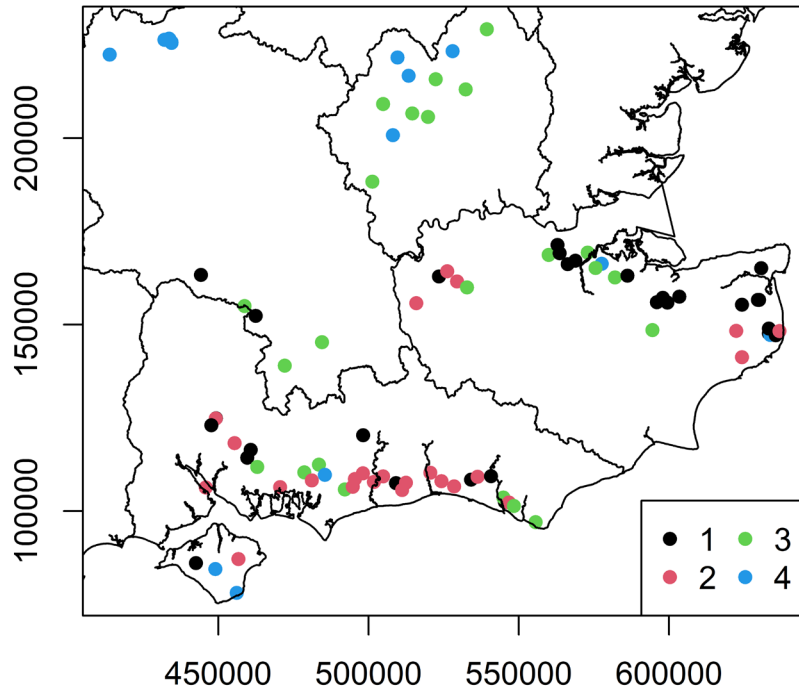


Figure 10 Spatial distribution of nitrate clusters overlain on EA areas. Uses WIMS data © Environment Agency copyright and/or database right 2023. EA areas © Environment Agency and/or database right 2016. All rights reserved.

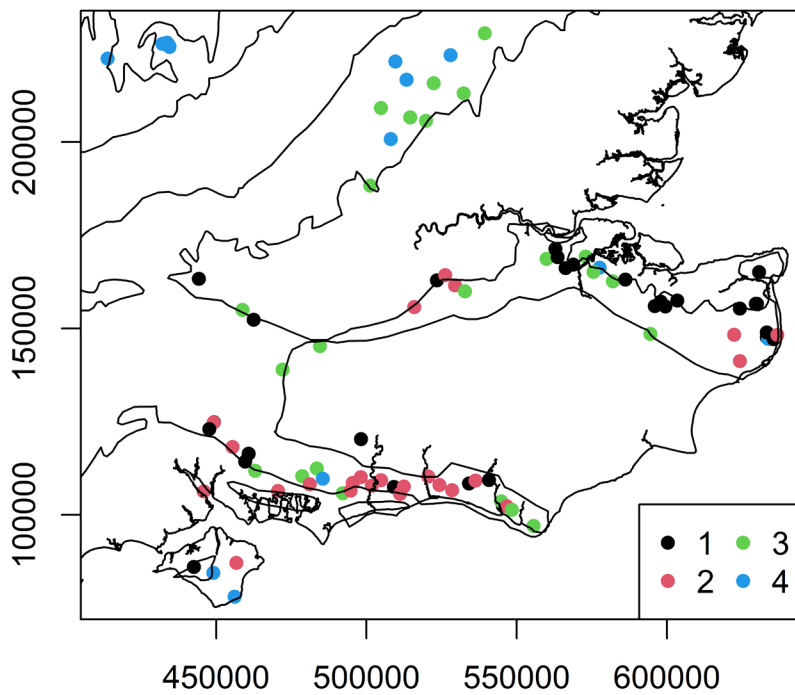


Figure 11 Spatial distribution of nitrate clusters overlain on 1:625,000 scale hydrogeological map. Uses WIMS data © Environment Agency copyright and/or database right 2023.

### 3.2.3 Evaluation of differences between clusters

Figure 12 shows the relationship between borehole depth and the four clusters. There is substantial overlap and no significant difference in the borehole depths between clusters 1 and 2. Boreholes in cluster 3 are significantly deeper ( $p < 0.05$ , one way analysis of means with unequal variances) than boreholes in cluster 4.

Figure 13 shows the correlation coefficients and lags for cross-correlations between detrended standardised monthly nitrate concentrations and monthly precipitation totals (left), groundwater levels (centre) and SGI (right), as split by cluster. Cluster 2 has strongest correlations with precipitation, GWL and SGI, followed by cluster 1. Clusters 3 and 4 are generally poorly correlated ( $r < 0.3$ ,  $p > 0.05$ ) with precipitation, GWL and SGI, with a wide range of lags for maximum correlation. For some sites in clusters 3 and 4 there were maximum correlations (albeit very weak,  $r < 0.3$ ) at negative lags. This has limited hydrogeological meaning and therefore these clusters are not considered further in these results.

For clusters 1 and 2, correlations between detrended standardised nitrate concentrations and GWLs are greater than for correlations with precipitation or SGI. Correlations with GWLs also appear to be less lagged in comparison to correlations with precipitation or SGI. There also appears to be less difference in the magnitude of the correlation coefficients between cluster 1 and cluster 2 when correlating with SGI in comparison to correlating with GWLs.

Figure 14 shows SPI-standardised nitrate correlations (left), SPI accumulation period (middle), and SPI lag (left) split across the four clusters. Cluster 2 has stronger correlations between SPI and standardised nitrate than cluster 1. Cluster 1 has greater magnitude and range of SPI accumulation periods and lags than cluster 2. This is also shown in Figure 15.

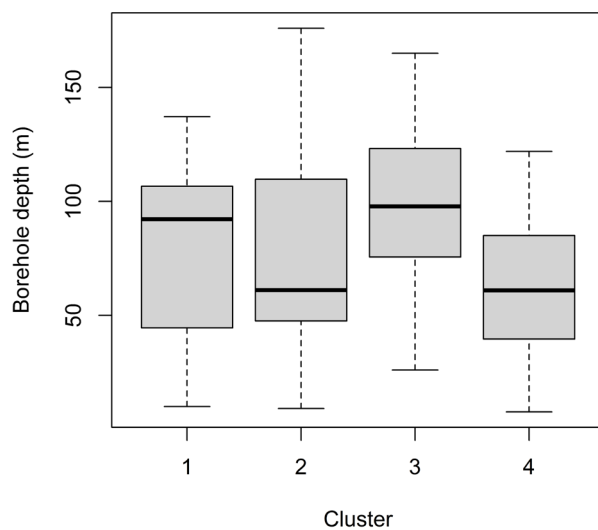


Figure 12 Boxplot of borehole depths for the different clusters

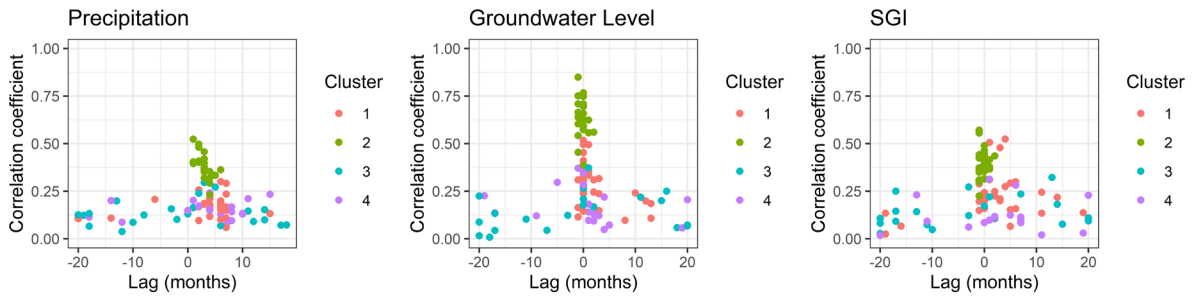


Figure 13 Maximum correlations and lags between standardised detrended monthly nitrate concentrations and monthly precipitation totals (left), monthly mean groundwater levels (centre), and standardised groundwater level index (SGI, right), split by cluster.

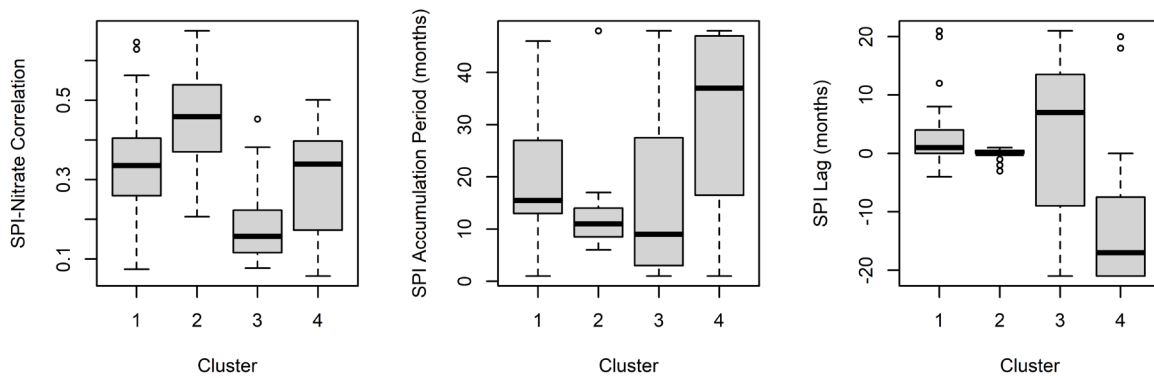


Figure 14 Boxplots of correlation (left), accumulation period (middle), and lag (left) for Standardised Precipitation Index (SPI)-standardised detrended monthly nitrate concentration correlations

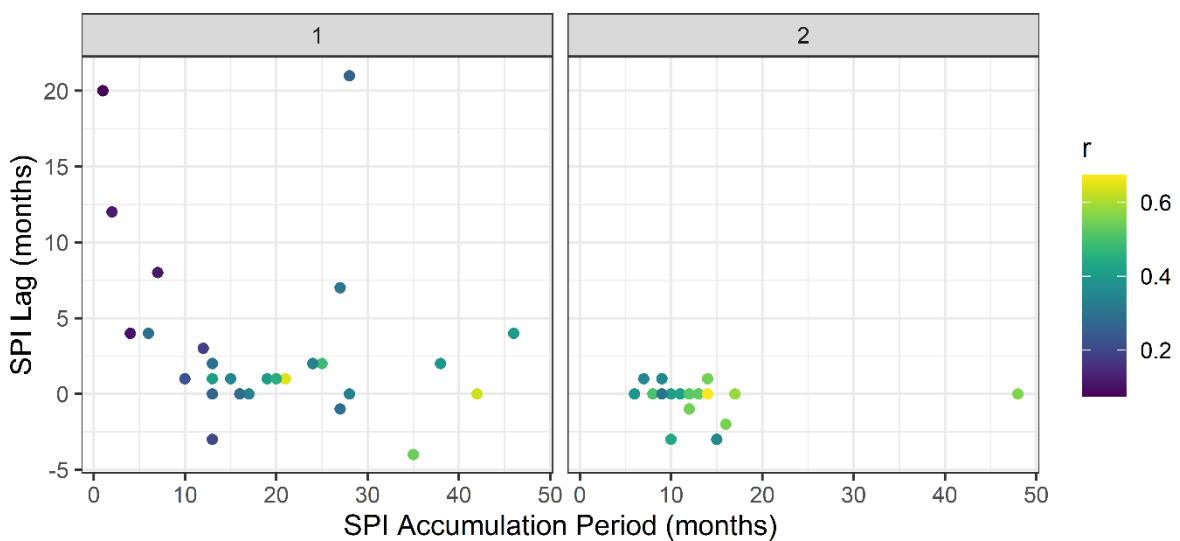


Figure 15 Standardised Precipitation Index (SPI) lags and accumulation periods for cluster 1 and 2 as a function of correlation coefficient  $r$ .

### 3.3 DISCUSSION

#### 3.3.1 WIMS nitrate data: the evidence base for historic climate change and suitability for assessment of the impacts of future change in southeast England

In phase 1 of this project Ascott et al. (2022), qualitatively highlighted the importance of long term records for assessment of climate change impacts on groundwater quality. In this report we have provided the first quantitative assessment at the regional-scale of the suitability of existing monitoring points for the assessment of climate change impacts on nitrate concentrations. This has highlighted the following:

- A small number of sites (19) meet the most stringent criteria (subset 1) for monitoring of climate change impacts based on guidelines by World Meteorological Organization (2017). These sites are only within the Chalk
- When applying slightly more lenient criteria (subsets 2 and 3), the number of sites increases substantially (96 and 284 sites respectively). This is dominated by the Chalk of southern England.

It should be noted that these results are based on an evaluation of an extract of the EA's WIMS database for southeast England for the determinands listed in section 3.1.1. In addition to this data, outside of southeast England, WIMS contains data for total oxidised nitrogen (TON, the sum of nitrate and nitrite). If the approach used here was to be upscaled to the national scale both TON in WIMS and any additional water company data that are currently not included in WIMS should be included.

Kendon et al. (2022) note that over 2012-2021, UK summers have been on average 6% and 15% wetter than 1991-2022 and 1961-1990 respectively. Over the same time periods, winters have been 10 and 26% wetter respectively. This increase in seasonal precipitation is within the range of natural variability in present climate. As a result of this and the relatively short length of records in subset 2 used in this analysis, the recent increase in seasonal fluctuations in cluster 2 cannot be directly attributed to climate change at present. Continued monitoring should be prioritised at the sampling points with the longest baseline records (as shown in top panels Figure 2) to provide context to possible future climate change impacts.

#### 3.3.2 Controls on historic temporal changes in groundwater nitrate fluctuations

The length of record and role of natural variability under current climate precludes direct attribution of climate change impacts on groundwater nitrate fluctuations. However, the analysis presented in section 3.2 does provide some insights into the overarching controls on historic temporal changes in groundwater nitrate fluctuations and the role of climate variability.

Clusters 3 and 4 show near-linear increasing and decreasing trends respectively. These trends appear to be controlled by depth of groundwater flow system intercepted by boreholes in each cluster. Boreholes in cluster 3 are significantly deeper ( $p < 0.05$ ) than cluster 4. In comparison to the deeper boreholes in cluster 3, the shallower boreholes in cluster 4 are likely to be intercepting groundwater flow with more rapid travel times due to thinner unsaturated zones and shorter saturated zone pathways. Consequently, it is likely that the increasing trends in the deeper boreholes reflect the "legacy nitrate peak" continuing to move through the unsaturated and saturated zone.

Superimposed on a long-term increasing trend, clusters 1 and 2 show non-linear and seasonal behaviour respectively. The timing of this behaviour is correlated to periods of high and low groundwater levels. There also appears to be some weak spatial coherence of the clusters with the majority of cluster 1 and 2 boreholes in the North and South Downs respectively. Differences in correlations with driving variables highlight the differences between clusters. Cluster 2 correlates strongest with groundwater levels, with notably



weaker correlations for cluster 1. However, when correlating with the “deseasonalised” SGI the differences in correlation strength between cluster 1 and 2 are small. When correlating detrended standardised nitrate concentrations with SPI, the strongest correlations for cluster 1 seem to be for longer accumulation periods and lags than for cluster 2. Marchant and Bloomfield (2018) showed that groundwater levels in the South Downs Chalk are notably flashier than in other regions (including the North Downs), associated with the high degree of faulting and fracturing (Jones and Robins, 1999). We suggest that the greater flashiness of groundwater level fluctuations in the South Downs is causing the seasonality in nitrate concentrations in comparison to the slower responding North Downs.

This poses the question, what processes are driving the seasonal fluctuations in cluster 2 and the non-linear behaviour in cluster 1? Stuart et al. (2009) identified 4 mechanisms that could control nitrate fluctuations in groundwater: (1) winter piston flow through the unsaturated zone matrix, (2) winter bypass flow from the base of the soil bringing high nitrate water directly to the water table, (3) water table rise from water entering elsewhere in the catchment flushing out porewater and (4) change in flow path giving access to a greater percentage of shallow high nitrate water. It was concluded that porewater flushing could potentially result in a lag between water table rises and nitrate concentration rises. As the strongest nitrate-groundwater level correlations for cluster 2 are for a lag of close to zero months (Figure 13 middle), it seems likely that mechanisms (3) can be ruled out. However, Stuart et al. (2009) also noted that without information such as unsaturated zone porewater concentrations, distinguishing between the other mechanisms is unlikely to be possible. Existing research has generally shown the bypass flow to be a relatively small component of total nitrate transport in the unsaturated zone. Using detailed nitrate sampling at the water table and porewater data, Sorensen et al. (2015) showed that for a site in the Hampshire Chalk, piston flow is the dominant mechanism, with winter bypass flow insignificant for nitrate fluctuations. Similarly, no evidence for bypass flow providing nitrate loads was observed in detailed site investigations in the Chalk of Northern France (Chen et al., 2019). If the same is true of the sites used in this research, it seems plausible that mechanism (2) can also be ruled out. Further, the requirement in this research to resample nitrate concentrations to monthly mean values means that short term, sub-monthly changes in nitrate that may be associated with bypass flow events may be “smoothed out”. The remaining mechanisms (piston flow and a changing flow path) are likely to be linked and will not be independent of each other.

### **3.3.3 Implications of variability between cluster 1 and 2 for future climate change impacts**

UKCP18 projections have a high confidence in wetter winters and drier summers (Met Office, 2018), and application of this data to lumped conceptual groundwater models produces a greater seasonal range in groundwater levels (Ascott et al., 2022). The temporal variability in sites in cluster 1 and 2 and the potential hydrogeological controls on this variability have important implications for how a “wetter winters drier summers” futures may affect future nitrate fluctuations.

Piston flow represents a transfer of energy from the land surface to water table. Any impacts of climate change on precipitation and recharge will be instantly transferred to the water table, with nitrate fluctuations controlled by legacy N in the unsaturated zone. Land use change impacts (either induced by climate change or otherwise) on N leaching will have a lagged impact on nitrate at the water table associated with travel times in the unsaturated zone.

In contrast, bypass flow represents the transfer of mass (of nitrate) from the land surface to the water table. In this mechanism, nitrate fluctuations may be due to current land use, and land use change impacts (induced by climate change or otherwise) on leaching may affect nitrate at the water table instantaneously.

Assuming piston flow and changing flow-paths are the dominant mechanisms controlling nitrate fluctuations, a greater seasonal range in precipitation due to climate change (and, by association, groundwater recharge and groundwater levels) would be expected to result in a greater range in nitrate concentrations. Nitrate concentrations at sites in cluster 2 would be expected to respond more rapidly than sites in cluster 1. This may mean that for a given series of precipitation events, groundwater levels and nitrate concentrations in cluster 2 may respond first and more rapidly than cluster 1. In contrast, recovery back to lower nitrate concentrations may be slower in cluster 1 than in cluster 2 as groundwater levels are less flashy in the former.

Under such climate change scenarios, a key factor is the relationship between the change in water level fluctuation and the legacy nitrate peak in the unsaturated zone. This is shown conceptually in Figure 16. Where the water table is on the rising limb of the unsaturated zone profile (left in Figure 16), increased seasonality in groundwater levels due to climate change will be associated with an increase in nitrate seasonality due to piston flow and changing flow-paths. It is likely this is what is currently occurring in cluster 2 at present. Where the water table is on the falling limb of the unsaturated zone profile (right in Figure 16), increased seasonality in groundwater levels will be associated with an increase in nitrate seasonality but with a shift in phase (i.e. when groundwater levels rise, nitrate concentrations decreases) in comparison to the rising limb. If there is no significant variation in nitrate across the range of water table fluctuation (Figure 16 middle) then no change in seasonality would be expected.

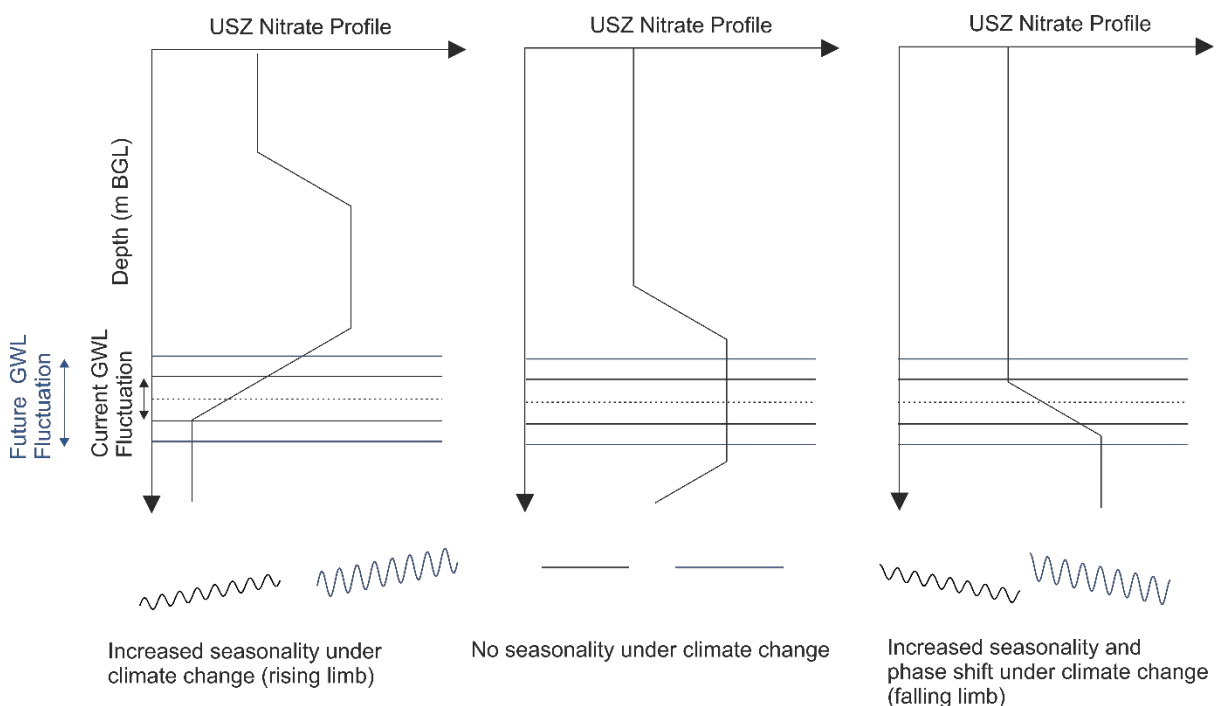


Figure 16 Simplified conceptual model of changes in nitrate fluctuations as a function of changing piston flow under climate change causing increased GWL fluctuation and varying unsaturated zone nitrate profiles.

### 3.3.4 Limitations and further work

The locations of the sites analysed are biased to the Chalk aquifer, and within the Chalk are further biased to public water supply abstractions which are typically located in river valleys. The cluster analysis approach adopted requires monthly data. As previously discussed, the

methodology cannot reveal and processes at a sub-monthly level, such as short term spikes which may be associated with bypass recharge events.

In this research it has not been possible to infer the exact balance of the different nitrate transport mechanisms for each site. Based on existing literature (Chen et al., 2019; Sorensen et al., 2015), we have had to make assumptions about the dominant processes controlling fluctuations (piston flow and changing flow-paths). Detailed information on porewater nitrate concentrations would be needed on a site-by-site basis to differentiate which processes are most important. Comparing the timescales for changes in precipitation, recharge, and groundwater level seasonality with the time for the legacy nitrate peak in the unsaturated zone to reach the water table would be a useful area to target further work.

Another alternative approach to collection of porewater data would be to combine the analysis of nitrate data with a determinant that is non-conservative in the unsaturated zone, such as microbial contaminants. Concurrent increases in microbial contaminants and nitrate may indicate that bypass flow is significant, whereas increases in nitrate without increases in microbial contaminants may indicate that piston flow is dominant. Such an analysis would require direct access to data collected by water companies, rather than indirectly via WIMS as has been undertaken here.

This case study has focussed on southeast England to demonstrate the methodology. As discussed in section 3.3.1, to upscale this approach nationally would require use of TON data and potentially data provided directly from water companies.

### 3.4 CONCLUSIONS

This research has analysed a large regional scale dataset of nitrate concentration time series using a combination of cluster analyses and standardised indices for the first time. The following conclusions can be drawn:

- The recent natural variability in climate combined with short record length means that any climate change impacts cannot be observed in the data provided.
- Cluster analysis has revealed different modes of temporal fluctuations in nitrate concentrations. The depth of groundwater flow system intercepted by the boreholes appears to control the long-term direction of change in groundwater nitrate concentrations.
- Non-linear and seasonal behaviour associated with climate variability are present in two clusters, which are weakly spatially coherent across the North and South Downs. Cross-correlation of nitrate time series with both raw and standardised indices of groundwater level and precipitation show that the extent of nitrate fluctuation appears to be controlled by precipitation and groundwater level fluctuation. This may be due to a combination of piston flow and changing groundwater flow paths.
- Under future climate change, nitrate fluctuations may change associated with the changing intersection of the water table and the legacy nitrate peak in the unsaturated zone.
- The timescales for land use change impacts on nitrate at the water table will vary substantially depending on the dominant process controlling nitrate fluctuations. Processes which represent a transfer of mass (bypass flow) will impact concentrations much more rapidly than processes representing a transfer of energy (piston flow).

## 4 Groundwater temperature analysis

### 4.1 METHODOLOGY

#### 4.1.1 Datasets

In this research, we build on the analysis of Ascott and McKenzie (2022), which analysed decadal scale groundwater temperature trends for a borehole in the superficial gravel aquifer in Wallingford. We have extended this analysis by incorporating data from a BGS research borehole on the Oxford floodplain previously studied by Macdonald et al. (2012), and data from groundwater temperature monitoring undertaken incidentally as part of level monitoring undertaken by water companies in England. A data request for in-situ groundwater temperature data recorded using loggers was made to 10 water companies in England. Data were only provided by Affinity Water. Affinity Water provided data for 29 sites in total. 11 of these sites could not be used due to evidence that the logger had been moved vertically within the borehole. For the remaining sites, individual logger files were compiled, and erroneous values (unrealistically high or low temperature values) were removed by visual inspection of each time series. For each site detailed metadata were also provided (location, borehole depth, depth of casing, depth of sensor). No other data were provided by water companies due either to lack of collection of groundwater temperature data from level monitoring, or lack of resources to provide the data to the timescales required for this project.

Across the data provided by Affinity Water and existing BGS data holdings, there are 20 groundwater temperature time series in total, covering both valley-bottom and deep interfluvial locations. The boreholes cover both superficial gravels and the Chalk. The boreholes are primarily in the Thames Basin in Southern England, with three gravel boreholes also located on the Dungeness Peninsula, Kent. Table 4 details the metadata for the sites.

In addition to the groundwater temperature time series, we also collated river and air temperature data for the catchment. Weekly river temperature time series for two sites (the Thames at Wallingford and Runnymede) were provided by UKCEH for 2007-2022 (an update of the publicly available data reported by Bowes et al. (2020)). Daily air temperature time series for three sites (Oxford, Benson, Rothamsted, Heathrow, Lydd Airport) were downloaded from the USA National Oceanic and Atmospheric Administration's Global Surface Summary of the Day (NOAA, 2022). The locations of the groundwater, river and air temperature time series are shown in Figure 17.

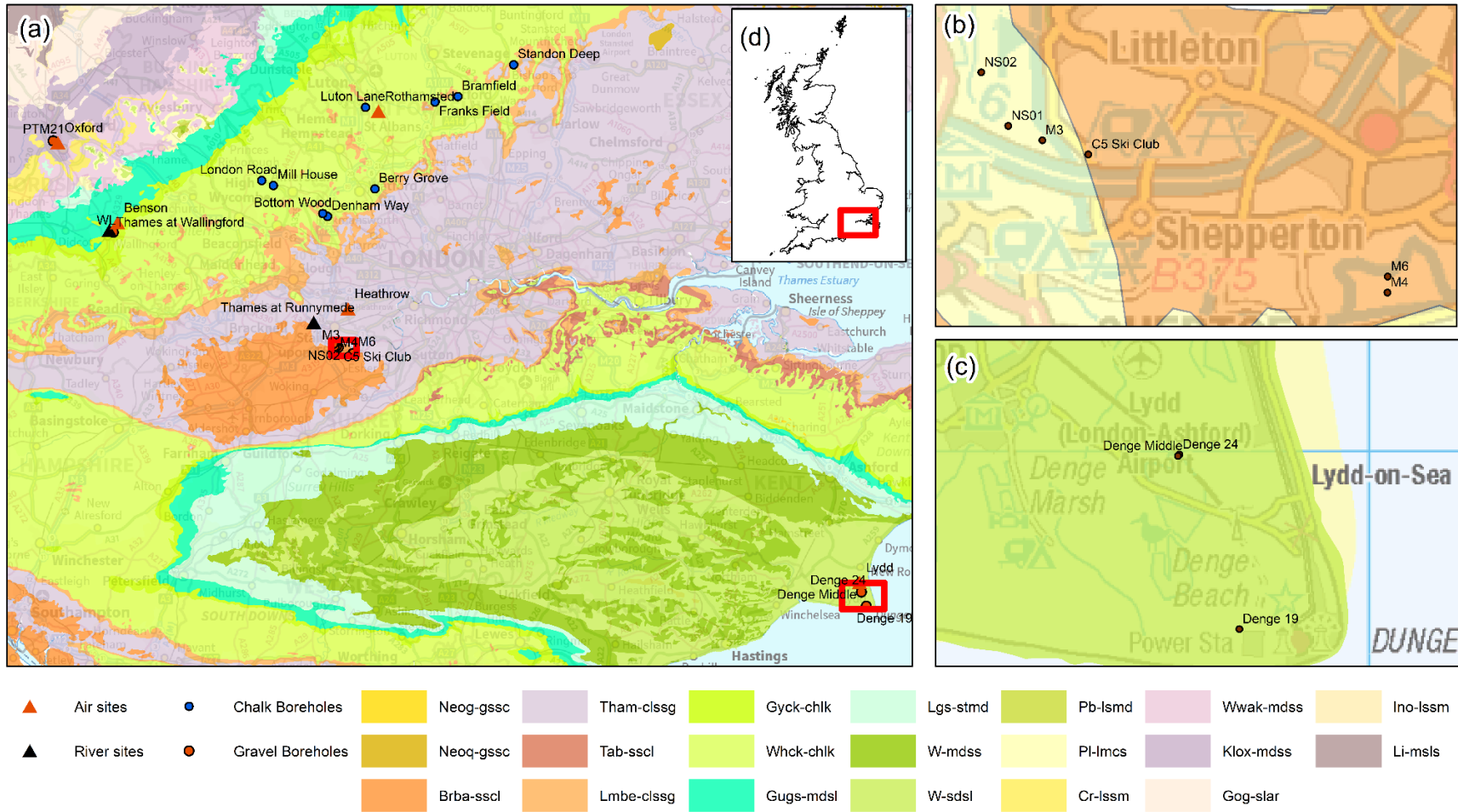


Figure 17 Location of groundwater, river and air temperature time series and 1:625,000 scale bedrock geology. Contains Ordnance Survey data © Crown copyright and database right 2023. Ordnance Survey Licence No. 100021290 EUL

Table 4 Metadata for groundwater temperature time series. Interfluve boreholes are marked with an asterisk. Affinity Water data © Affinity Water.

Name	Data source	Easting	Northing	Datum (mAOD)	Borehole Depth (m)	Casing Depth (m)	Sensor Depth (m)	Aquifer	Associated river temperature site	Associated meteorological site
PTM21	BGS	449993	207525	57.00	1.4	0.3	1.2	Gravel	Thames at Wallingford	Oxford
WL		461690	189790	46.00	5	4	4.5	Gravel	Thames at Wallingford	Benson
C5 Ski Club		505393	167414	13.04	12	2	12	Gravel	Thames at Runnymede	Heathrow
M3		504956	167549	12.50	12	2	6	Gravel	Thames at Runnymede	Heathrow
M4		508249	166097	10.46	12	2	6	Gravel	Thames at Runnymede	Heathrow
M6		508251	166249	10.12	12	2	6	Gravel	Thames at Runnymede	Heathrow
NS01		504630	167686	13.57	12	2	12	Gravel	Thames at Runnymede	Heathrow
NS02		504373	168197	12.80	12	2	12	Gravel	Thames at Runnymede	Heathrow
Denham Way*		503300	192860	46.94	24.38	7.16	6.3	Chalk		Rothamsted
Berry Grove		512491	198199	60.29	10	2	10	Chalk		Rothamsted
Denge 19	Affinity Water	607949	117199	5.72	9.1	9.1	6	Gravel		Lydd
Denge 24		607005	119944	4.91	6.5	6.5	5	Gravel		Lydd
Denge Middle		606982	119921	4.90	7.1	7.1	5	Gravel		Lydd
Franks Field		524175	215074	61.97	8.5	6.5	8	Chalk		Rothamsted
Bottom Wood*		502370	193420	66.18	100	20	10.7	Chalk		Rothamsted
London Road		490500	199820	115.70	15	10	7.5	Chalk		Rothamsted
Luton Lane		510677	214038	101.09	14	9	13.5	Chalk		Rothamsted
Mill House	492781	198866	104.34	17	12	9.8	Chalk		Rothamsted	
Standon Deep	539443	222289	63.38	50	19	11	Chalk		Rothamsted	
Bramfield*	528612	216118	94.90	150	25	52	Chalk		Rothamsted	

### 4.1.2 Analytical approach

We analysed the groundwater, river and air temperature data using a combination of visual and time series analysis techniques.

We first plotted the groundwater temperature time series in the time domain. The seasonal and diurnal cycle in groundwater temperature time series for each site were plotted. For sites that showed evidence of diurnal fluctuations the time series in the frequency domain were plotted.

We then extracted several metrics to describe the properties of each groundwater temperature time series. The linear trend in each time series was calculated using a linear model accounting for seasonal fluctuations. This is the same method as used by Ascott and McKenzie (2022). We also used this method to calculate the trend in the river and air temperature time series. The seasonal range in the groundwater temperature time series was extracted. Lagged cross-correlations between groundwater temperature time series and local air temperature time series were calculated (the air temperature sites are shown in Figure 17, and Table 4 shows which air temperature site corresponds to each borehole). For each site we recorded the lag and correlation coefficient that corresponded to the maximum correlation between groundwater temperature and air temperature.

To explore the controls on groundwater temperature fluctuations between the sites, the time series metrics were correlated with metadata describing the hydrogeological setting of the sites (borehole depth, casing depth, depth of sensor, as shown in Table 4). We used these results to explore controls on the temporal changes in groundwater temperatures at the sites, and evaluated the implications of this for changes in groundwater temperature and other aspects of groundwater quality under climate change.

## 4.2 RESULTS

### 4.2.1 Near-decadal, seasonal and diurnal variability in groundwater temperature time series

Figure 18 shows the compiled groundwater temperature time series for the 20 sites. The length of record for the sites is variable. The time series data provided by Affinity Water are often from c. 2014 to date, although some sites start earlier (e.g C5 Ski Club, NSO1). The data for PTM21 in Oxford cover an earlier period from 2003-2017, and are therefore also shown in detail in Figure 19.

There are clear differences between the sites in the magnitude of seasonal fluctuations in groundwater temperature. The shallower boreholes (e.g. PTM21, WL, Denge) appear to have greater seasonal fluctuations than the deeper boreholes, in particular those in interfluvial settings (Denham Way, Bramfield, Bottom Wood). PTM21 also shows evidence of non-linear trends in groundwater temperature, with an increase over 2003-2006, a decrease over 2006-2011, and an increase over 2011-2017 (Figure 19).

Figure 20 shows the compiled groundwater temperature time series for the sites excluding PTM21 (due to the lack of overlapping data in time), with each site plotted on separate y axes for clarity. Visually there is an increasing trend at many of the sites, including in deeper boreholes at interfluvial locations (Bottom Wood, Bramfield, Denham Way). However, several sites (Franks Field, London Road, M3, NSO1) show limited trends over time.

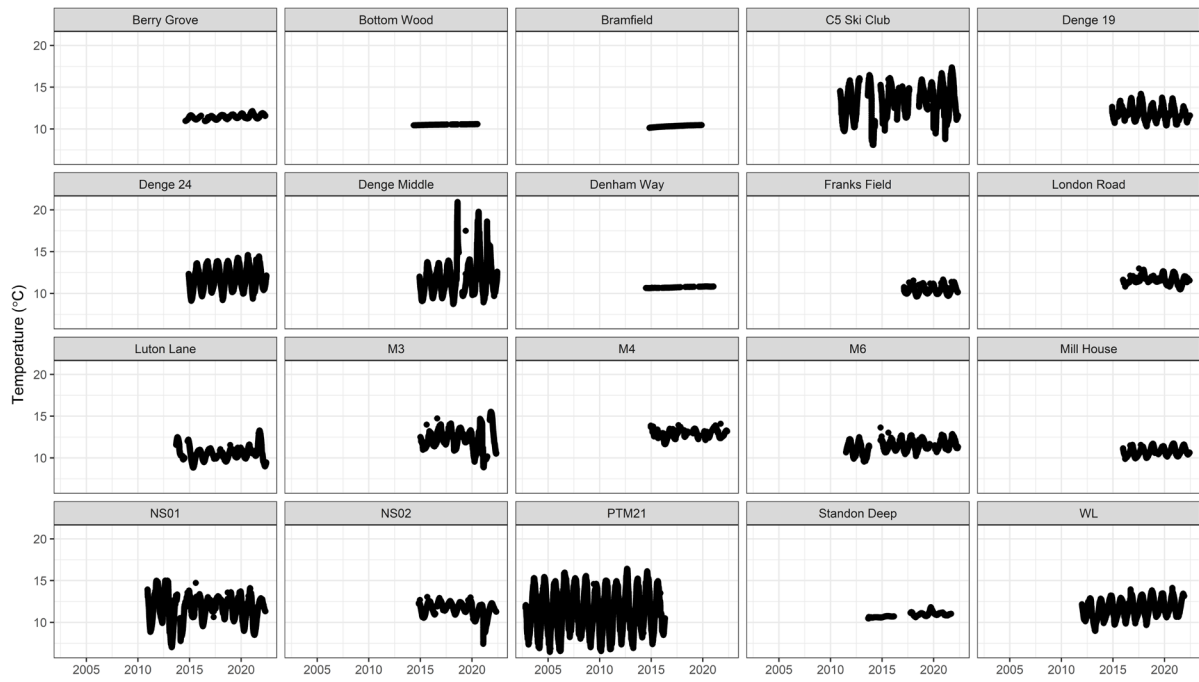


Figure 18 Groundwater temperature time series for BGS and Affinity Water sites. Affinity Water data © Affinity Water.

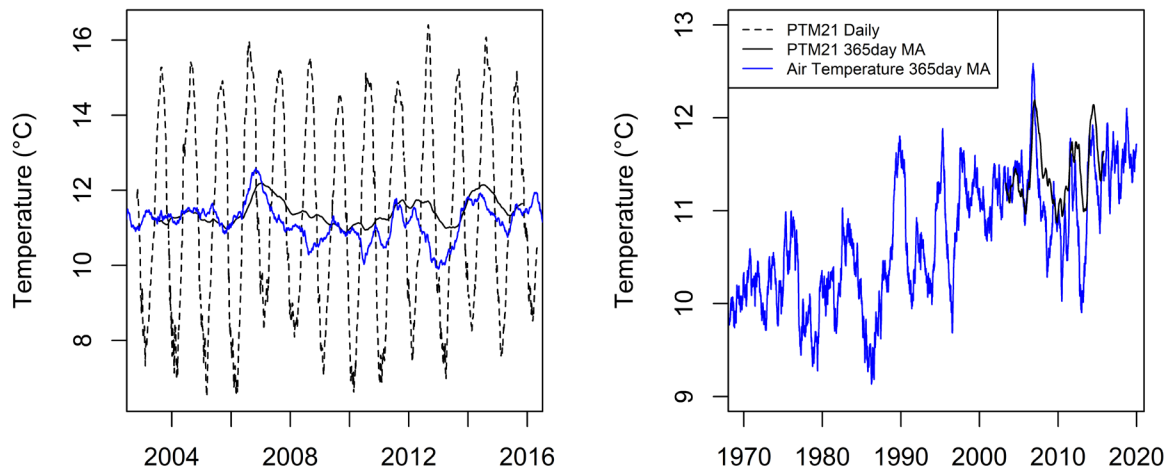


Figure 19 Groundwater temperature time series at PTM21 and air temperature time series at Oxford for 2003-2017 (left) and 1970-2020 (right). Air temperature data reproduced from Burt and Burt (2019)



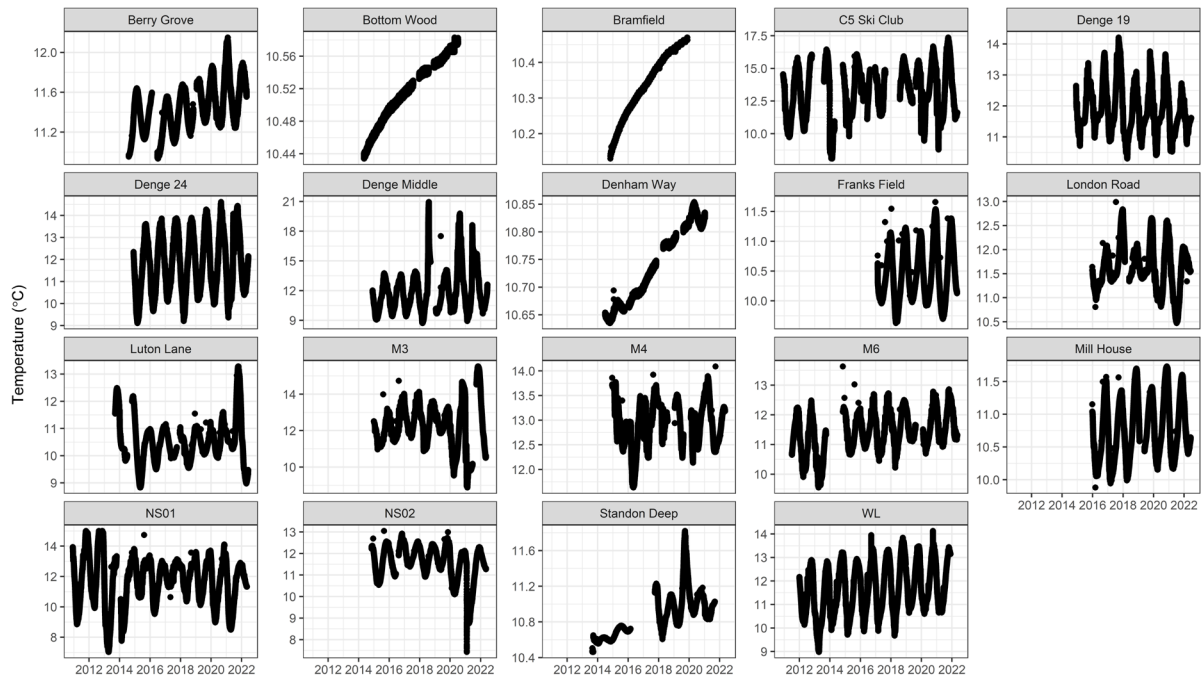


Figure 20 Groundwater temperature time series for BGS and Affinity Water sites. Each site is plotted on individual y-axis scales and PTM21 has been removed for clarity. Affinity Water data © Affinity Water.

Figure 21 shows the seasonal cycle in groundwater temperature for each site. There are differences in the magnitude and timing of the seasonality in groundwater temperatures. The interfluve sites (Bottom Wood, Bramfield and Denham Way) show no seasonal variability. Sites with the greatest seasonal variability (PTM21, Denge Middle, C5 Ski Club) have a seasonal temperature peak earlier than those with a smaller seasonal variability (e.g. Luton Lane, WL, Denge 24).

Figure 22 shows the diurnal cycle in groundwater temperature for each site. Most sites show no diurnal variability, or any variability is controlled by sensor resolution (C5 Ski Club, NS01). Denge 24, Denge Middle and WL show diurnal cycles in groundwater temperature, with decreases in the morning and increases in the afternoon. This diurnal variability is also evident when plotting the data for these sites in the frequency domain (Figure 23). A distinct spike in the power spectrum is present at frequency = 365 (i.e. a diurnal cycle) for the three sites.

Figure 24 shows the diurnal cycle for these sites stratified by season. For each site the diurnal cycle varies between season. The greatest diurnal range is in summer (June July August (JJA)), where all three sites show increases from c. 9 am to 7 pm. The smallest diurnal range is generally in spring and autumn (March April May (MAM) and September October November (SON)). In these months Denge 24, WL and Denge Middle in spring show increases from c. 1 am to c. 7 pm. In contrast Denge Middle shows a decrease over the same time period in Autumn, albeit at a lower rate in comparison to between 1 am and 10 am. The same pattern of a change in the rate of decrease in groundwater temperature through the day is also observed in winter at WL and Denge Middle.

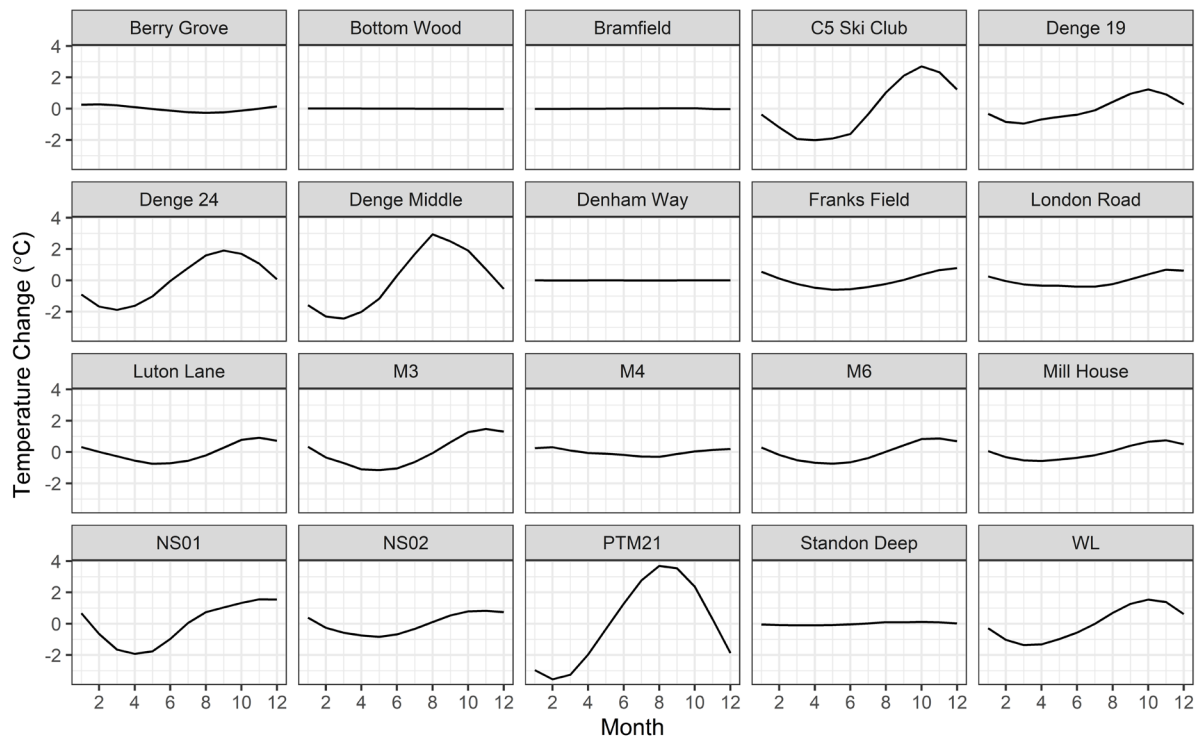


Figure 21 Seasonal cycle in groundwater temperature time series. Affinity Water data © Affinity Water.

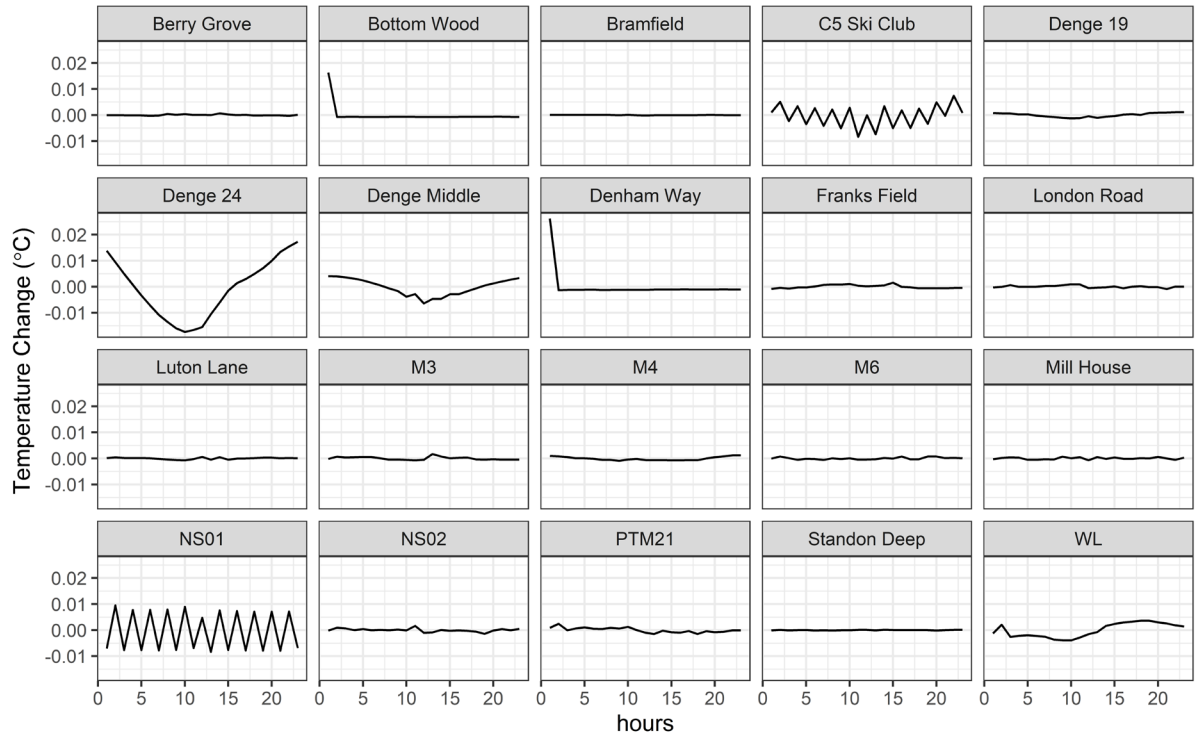


Figure 22 Diurnal cycle in groundwater temperature time series. Affinity Water data © Affinity Water.

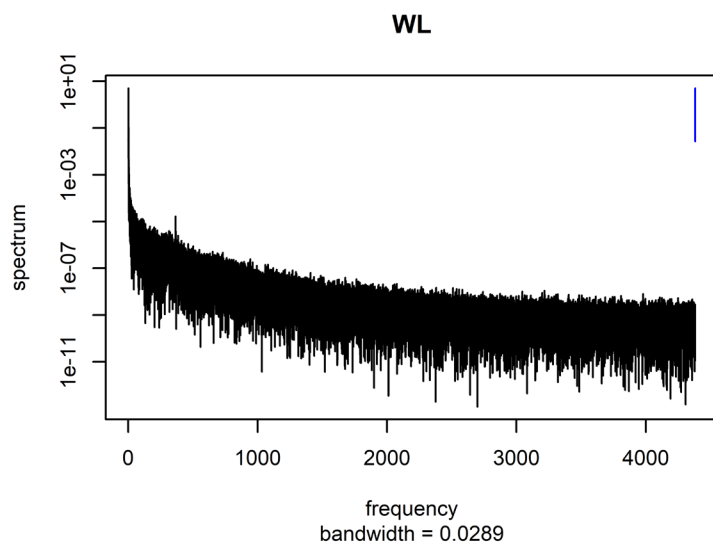
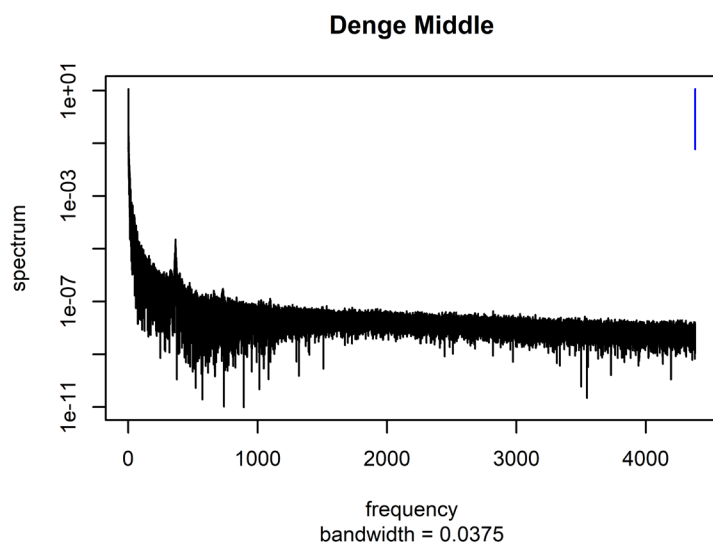
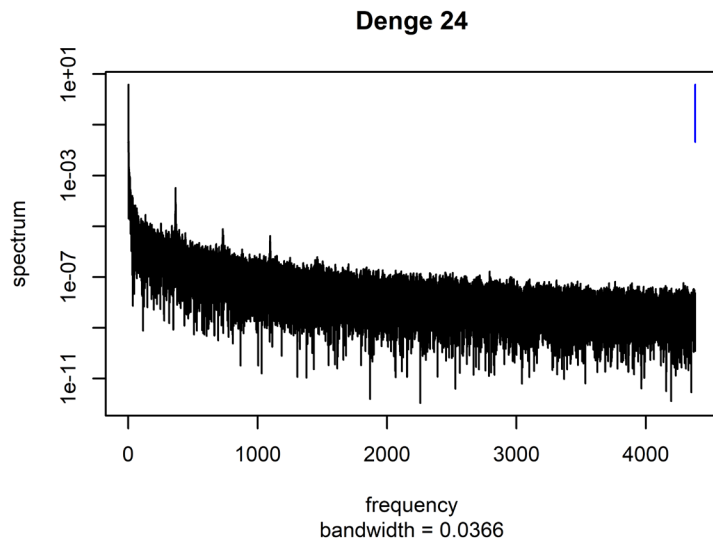


Figure 23 Groundwater temperature time series in the frequency domain

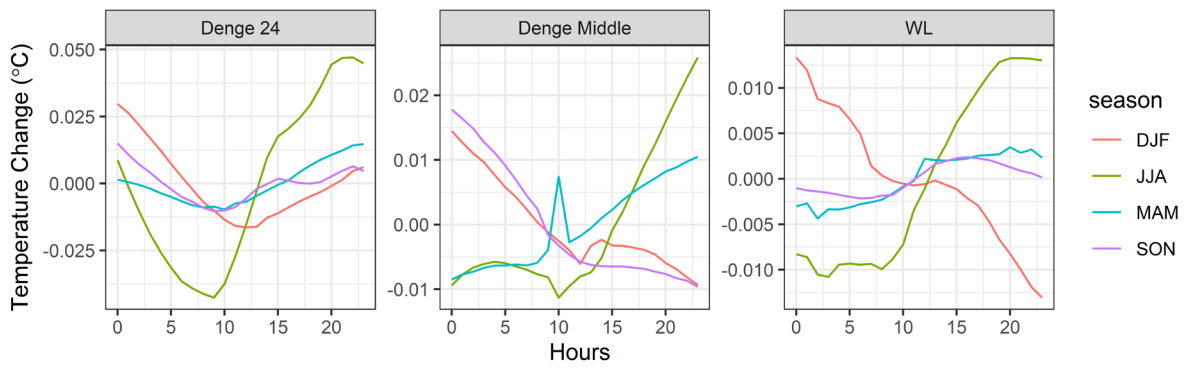


Figure 24 Diurnal cycle in groundwater temperature time series at Denge 24, Denge Middle and WL stratified by season. Affinity Water data © Affinity Water.

#### 4.2.2 Trends in groundwater temperature time series

Figure 25 shows the trends in groundwater, river and air temperature data over 2012-2022. Groundwater temperature trends are variable across the sites. Increasing trends occur in 75% of sites. The mean trend across all sites over 2012-2022 is  $+0.40$  °C/decade, and across the sites showing increases the mean trend is  $0.68$  °C/decade. River temperatures show increasing trends of c.  $1$  °C/decade over 2012-2022, with trends of a similar magnitude at the nearest groundwater temperature sites (C5 Ski Club, WL). Air temperatures are also rising at 4 out of the 5 sites by c.  $1$  °C/decade. One air temperature site (Lydd) shows a slight decreasing trend which is also observed at nearby Denge 19 borehole, but not at Denge Middle and Denge 24.

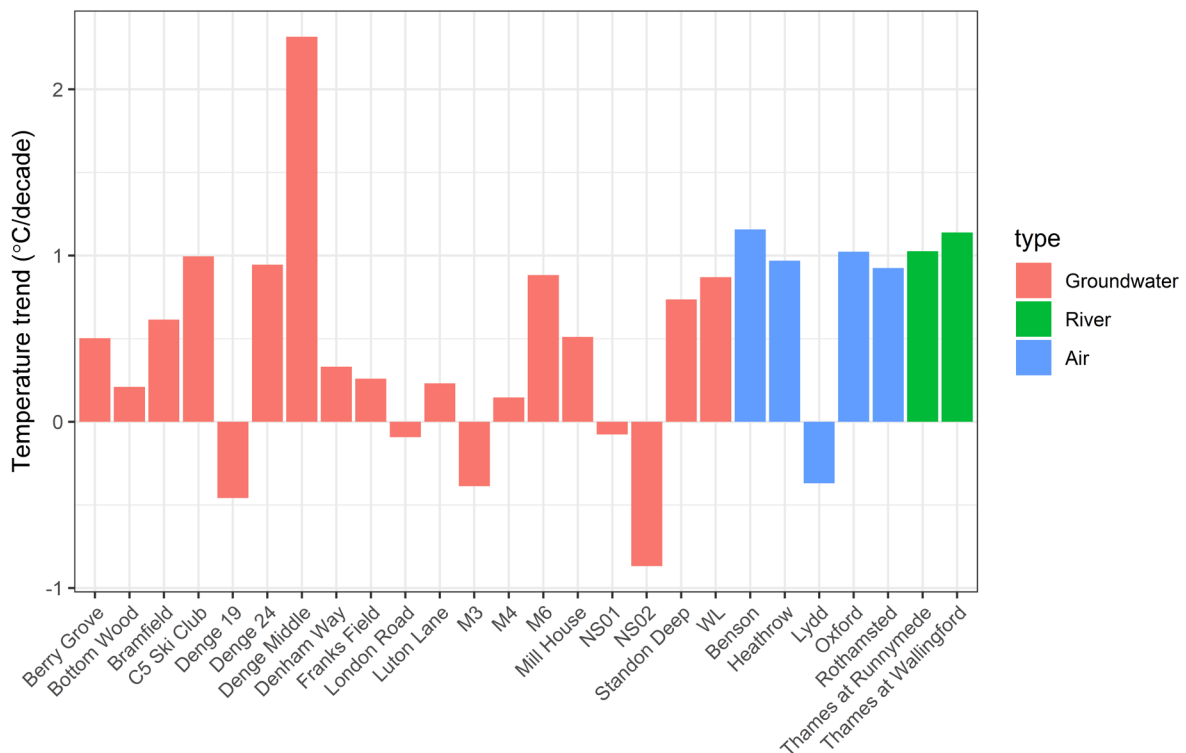


Figure 25 Trends in groundwater, air and river temperature time series. Affinity Water data © Affinity Water.

### 4.2.3 Relationships between metrics of groundwater temperature time series and borehole hydrogeology

Figure 26 shows relationships between the metrics calculated for each groundwater temperature time series and information regarding the hydrogeology of each borehole (borehole depth, casing depth, sensor depth). Seasonal groundwater temperature range is significantly negatively correlated with the depth of borehole and casing ( $p < 0.05$ ). Visually, seasonal groundwater temperature range is negatively correlated with depth of sensor however this correlation is not statistically significant ( $p > 0.05$ ).

There is no correlation between groundwater temperature trend and depth of borehole, casing or sensor ( $p > 0.05$ ). The strength of the correlation between groundwater temperature and air temperature is significantly negatively correlated with the depth of borehole, casing or sensor ( $p < 0.05$ ). There is no correlation between lag for the best correlation between groundwater and air temperature and depth of borehole, casing or sensor ( $p > 0.05$ ).

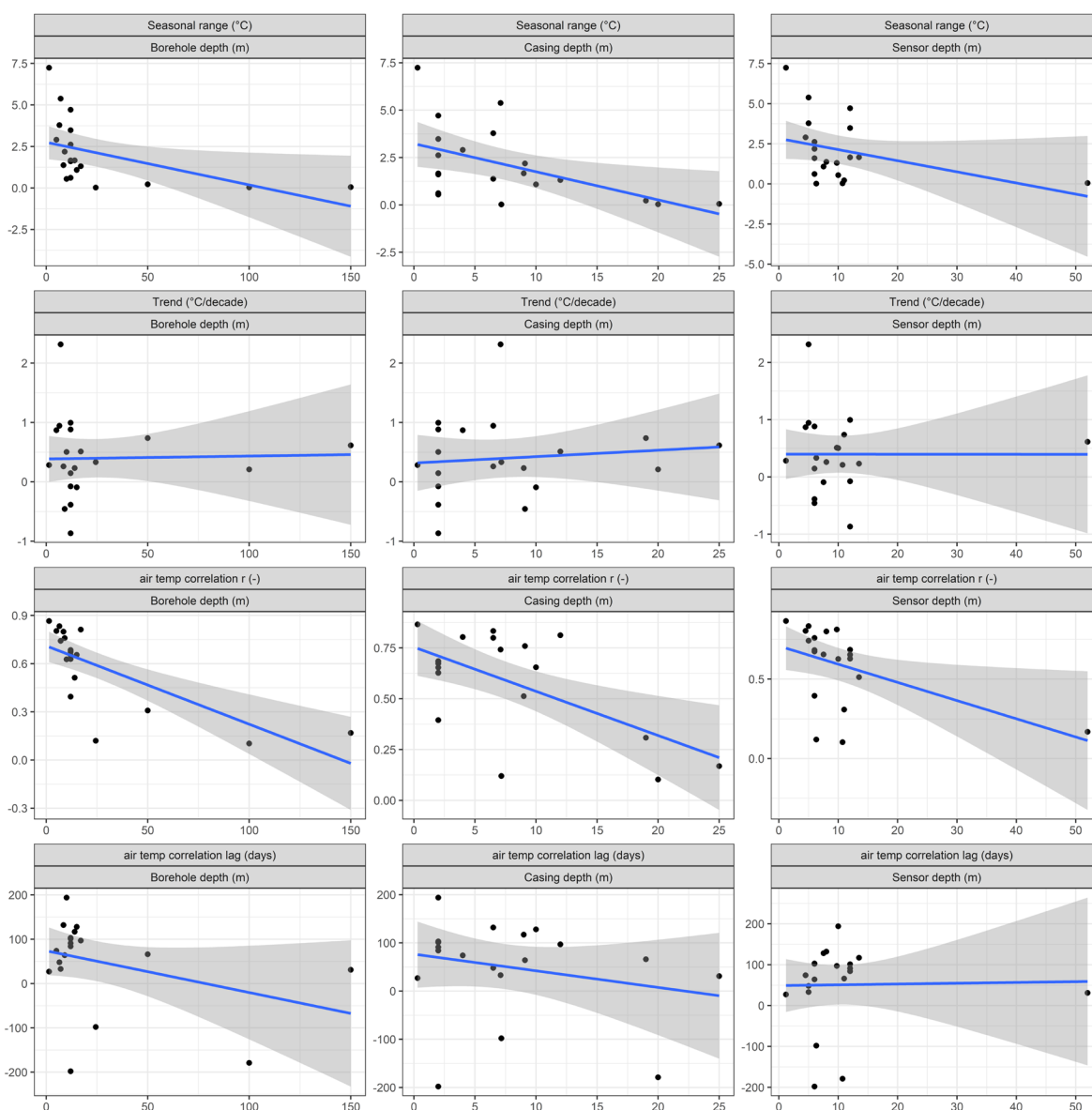


Figure 26 Correlations between time series metrics and metadata. Affinity Water data © Affinity Water.

## 4.3 DISCUSSION

### 4.3.1 Controls on observed groundwater temperature fluctuations

The analysis presented in section 4.2 has shown groundwater temperatures to fluctuate on a range of temporal scales. The likely controls on the observed groundwater temperature changes are assessed below.

All 20 sites are rural or peri-urban, and there have been no significant changes in local land use over the past 20 years based on a comparison of the UKCEH landcover mapping for 2007 and 2021 (Marston et al., 2022; Morton et al., 2014). We therefore consider it unlikely that observed temperature trends are controlled by large-scale increases in the urban heat island effect, as has been observed in heavily urbanising areas worldwide (Zhu et al., 2015). We postulate that a first order control on near-decadal scale temperature trends in shallow boreholes is current air temperature trends. In permeable formations, air temperature signals are known to propagate into the shallow subsurface through a balance of conduction and advective heat transport by groundwater flow (Taylor and Stefan, 2009). The control of shallow groundwater temperature trends by air temperature is evident at several sites. For example, PTM21, where GWT data cover a different time period to the other sites, shows a temporary temperature decline over 2006-2011, before rising again. This is also observed in air temperature time series for Oxford over the same period (Figure 19), and seasonal groundwater temperature peaks lag behind air temperature peaks by c. 30 days in this very shallow borehole. The variable and relatively short record length makes direct comparison of trends between the sites challenging and, in some cases, affected by individual years where temperatures are particularly high or low. Berry grove, C5 ski club, WL, M4, M6, Standon Deep and Mill House all show increasing trends in groundwater temperature at near-decadal time scales that are relatively consistent with increasing local air temperature trends over the same period. It is interesting to note that rates of increase in groundwater temperature are somewhat lower than rates of increase in river temperatures (Figure 25). In addition to the variable record length, the slightly weaker coupling of air and groundwater temperature compared to air and river temperature may also be due to energy losses of the air temperature signal during propagation through the subsurface. Interestingly, Denge 19 shows a decreasing trend which is consistent with the observed decrease in temperature at the local air temperature site at Lydd. These trends at Denge 19 and Lydd are principally associated with anomalously high air temperatures in 2014-16 relative to the other air temperature sites (see seasonal anomaly maps shown in Kendon et al. (2015)), followed by lower temperatures in subsequent years.

The remaining shallow groundwater temperature sites show either weak positive trends (Franks Field, Luton Lane, M4), weak negative trends (M3, NS01, NS02) or strongly positive trends in absence of an increasing local air temperature trend (Denge 24, Denge middle). For these sites we posit that groundwater temperature trends are a function of a complex balance of changes into heat fluxes into the subsurface associated with a range of possible heat sources, superimposed upon changes in groundwater flow to the borehole associated with recharge and discharge processes. It is beyond the scope of this research to provide a detailed process-based evaluation of the sources of heat to each of these boreholes. Whilst no significant large-scale land use change has been observed based on land cover mapping, this does not preclude the influence of highly localised changes in land use which could change heat fluxes into the subsurface. Such local heat sources could include anthropogenic activities such as ground source heating and cooling schemes, wastewater discharges, increased paved surfaces, in-ground heat losses from buildings and shallow subsurface infrastructure (Zhu et al., 2015).

The three deep interfluvial boreholes (Bottom Wood, Denham Way, Bramfield) also show near-decadal scale increasing trends. For these sites, given their hydrogeological setting, we postulate that groundwater temperature trends are controlled principally by historic air temperature trends and propagation of this signal by conduction to the borehole at depth (assuming thermal equilibrium between the rock matrix and groundwater). At present the “age” of the temperature signal being observed in these boreholes is unknown, but it is interesting to note that the increasing trend observed at both Bottom Wood and Bramfield appears to be levelling off in recent years (Figure 20).

The extent of seasonal fluctuation in groundwater temperatures appears to be primarily a function of borehole depth, casing depth and sensor depth. Shallower boreholes show the greatest seasonal fluctuation. The cause of seasonal fluctuations in shallow groundwater temperatures is likely to be seasonal fluctuation in air temperatures (Taylor and Stefan, 2009). Propagation of the air temperature signal into the subsurface is likely to be via conduction and advective heat transport by groundwater flow. These processes are consistent with the posited drivers of decadal scale temperature trends in shallow boreholes. This is also supported by the stronger correlations between air temperatures and groundwater temperatures at the shallowest sites (Figure 26).

The diurnal cycles observed in groundwater temperature at Denge 24, Denge Middle and WL (Figure 24) are within ranges that are below the level of accuracy of the sensor (typically 0.1 °C). Consequently, the magnitude of these cycles should be treated with caution. The presence of diurnal cycles in observations of groundwater temperature is principally controlled by depth, accuracy and resolution of the sensor. Denge 24, Denge Middle and WL are, except for PTM21, the shallowest boreholes with the shallowest sensors (Table 4). PTM21 only consistently records groundwater temperature to 2 decimal places, and thus variations below 2 decimal places as shown in Figure 22 have not been observed. When splitting the diurnal groundwater temperature cycle by season this shows the greatest range in summer. Increases in temperature start from c. 9 am daily. It is likely that the diurnal changes observed are controlled by a combination of propagation of diurnal air temperature variability, and diurnal evapotranspiration from groundwater changing the water balance of inflows to the boreholes.

#### **4.3.2 Observed groundwater temperatures and climate change**

This research has shown that several shallow boreholes have near-decade scale increases in groundwater temperature. One shallow site also shows evidence of non-linear decadal scale trends (PTM21), and deep interfluvial boreholes also show increases. These trends are likely to be controlled by current air temperature trends for the shallow sites and historic air temperature trends for the deep sites.

Given the length of the groundwater temperature time series, and potential other sources of heat fluxes into the subsurface, it is not possible to directly attribute the recent GWT trends directly to climate change. Over the period where groundwater temperatures have been monitored (2012-2021), annual mean air temperatures for England have been over a degree warmer than the 1961-1990 average (Kendon et al., 2022). Given the control of local air temperature on shallow groundwater temperatures, it is therefore likely that shallow groundwater temperatures have increased in previous decades in line with historical climate change. In the future, it is likely that shallow GWT will continue to change as a function of air temperature variability associated with climate change. UKCP18 projections (Met Office, 2018) show greater warming in summer than winter, with the greatest temperature increases in southern England. It is therefore likely that future climate change will result in long term increases in groundwater temperature and increases in seasonality. Diurnal temperature cycles in shallow boreholes have also been shown to vary between seasons (Figure 24), and so any changes in seasonality due to climate change may also affect diurnal responses.

#### **4.3.3 Implications for other aspects of groundwater quality and surface water ecosystems**

Both the historic observed increasing trend in groundwater temperatures for some boreholes and future changes are likely to have implications for other aspects of groundwater quality. For groundwater in England, there is limited empirical evidence for relationships between increasing groundwater temperature and other groundwater quality variables. However, the international peer-reviewed literature provides some insights into what potential changes in groundwater quality variables may occur as a function of increasing groundwater temperatures.

Riedel (2019) demonstrated that a 1 °C rise in groundwater temperature resulted in increased microbial respiration and mineralisation of organic matter. This was shown to result in a 4% decline in dissolved oxygen saturation, a pH decrease of 0.02 associated due to increased pCO<sub>2</sub>, and increased DOC and Mn in groundwater due to more reducing conditions. Similar conclusions regarding temperature controls on groundwater DOC were also drawn by

McDonough et al. (2020). Riedel (2019) went on to suggest that decreases in dissolved oxygen saturation due to groundwater temperature changes may affect groundwater fauna such as stygobites. This in turn may affect ecosystem services they provide (e.g. grazing of biofilms, biogeochemical cycling with bacteria (Maurice and Bloomfield, 2012)).

The combination of increasing temperature and decreasing dissolved oxygen has been shown to increase denitrification (Gervasio et al., 2022; Veraart et al., 2011), although it likely this will remain limited to within soils, confined aquifers and hypoxic zones (Rivett et al., 2008). Bloomfield et al. (2006) and Cavelan et al. (2022) highlighted that increases in temperature would result in increases in degradation of pesticides and NAPLS respectively in soils and groundwater. If degradation is aerobic, then decreases in dissolved oxygen saturation may offset any increases due to increased temperature.

The potential changes in groundwater quality above are largely a function of long-term groundwater temperature changes. Increased seasonal fluctuations in shallow groundwater temperature may also affect other components of groundwater quality in the short term. As long-term groundwater temperature increases appear to be occurring in both Chalk and gravel aquifers, and in shallow valley bottom and deep interfluvial settings, it is plausible that groundwater quality changes may be occurring across these settings.

The observed increases in groundwater temperatures also have important implications for surface water ecosystems. Groundwater temperatures are typically cooler than surface water in summer months and warmer during winter months. Groundwater discharge to surface water bodies therefore buffers diurnal and seasonal variability in surface water temperatures. This is particularly important in summer months, where discrete groundwater discharges have been shown to provide hydro-refugia for cold-water species (Hayashi and Rosenberry, 2002). Increasing groundwater temperatures observed in this research may result in refugia being less habitable for cold-water species. Worrall et al. (2022) showed that river temperatures in the UK are not rising as fast as air temperatures. They argued that one reason for this is buffering by groundwater discharges to surface waters, and they note that under future climate change that this buffering may break down. Whilst the trends observed in our research are relatively small (<1 °C/decade), the increases in groundwater temperature provide some initial limited evidence that the breakdown of such buffering is likely to have already begun.

#### 4.3.4 Recommendations for future work

In this research we have not evaluated detailed local-scale processes that control groundwater temperature fluctuations for each site individually. Such an assessment would be required as a precursor to modelling the GWT time series using statistical or analytical models. These models could then in turn be used to develop reconstructions and future projections of groundwater temperature as a function of climate variability and change.

The data collected by Affinity Water represents incidental monitoring of groundwater temperature where the main purpose is to monitor groundwater levels. This work has highlighted the value of such incidental monitoring in the characterisation of temporal changes in groundwater temperature. It would therefore be a worthwhile activity to undertake further groundwater temperature “data rescue” from other water companies or the Environment Agency to determine how widespread the groundwater temperature variability observed in this research is. Further, given the limited additional resource required to collect temperature data from groundwater level loggers that measure temperature as standard it is recommended that where existing loggers are in-situ that temperature recording is “turned on”, and that this data is collated as standard practice.

For the development of future intentional groundwater temperature monitoring, this research has highlighted several key considerations. The depth of borehole and sensor is a key control on the extent of diurnal and seasonal fluctuation, and the “age” of the temperature signal being observed in the borehole. The accuracy and resolution of sensors deployed is dependent on the scale of groundwater temperature fluctuations of interest. For example, intentional monitoring of diurnal cycles in groundwater temperature as observed in Figure 24 would require sensors with a resolution and accuracy of 0.001 °C. Development of site-specific conceptual models of potential controls on groundwater temperature is an overarching requirement to



support both the most appropriate monitoring installations and to support interpretation of the data collected.

#### 4.4 CONCLUSIONS

This research has evaluated whether groundwater temperatures are increasing as a function of climate variability and change, as well as explored how groundwater temperatures vary across different temporal scales and depths. The following conclusions can be drawn:

- At 8 of 16 shallow boreholes with temperature data over 2012-2022, groundwater temperature trends are broadly consistent with current air temperature trends. 7 of these sites show increasing trends, with a mean trend of 0.66 °C/decade. Three deep interfluvial sites show increases, with a mean trend of 0.38 °C/decade. It is likely that these trends are controlled by current and historical near-decadal trends in local air temperature for shallow and deep sites respectively.
- The remaining 8 shallow sites show inconsistent trends in comparison with local air temperature trends. For these sites it is likely that in addition to air temperature trends, additional heat fluxes into the subsurface are occurring superimposed on changes in groundwater flow to the boreholes.
- The shallow sites show seasonal temperature fluctuations associated with propagation of air temperature signals, with seasonal range in groundwater temperature significantly negatively correlated with borehole depth. Three very shallow sites show diurnal fluctuations, although these fluctuations are below the accuracy of the sensors.
- The increases in groundwater temperature observed have some implications for other components of groundwater quality (e.g. biogeochemical cycles, stygobites, pollutant (N, pesticide, LNAPL) degradation and for the role that groundwater discharges to surface water play in providing cold-water hydro-refugia to cold-water species during summer.

## References

- Ascott, M., Lewis, M., Goody, D., Mackay, J., Smedley, P., Cartwright, C., 2022. Impacts of Climate and Land Use Change on Groundwater Quality in England: A Scoping Study, British Geological Survey, Keyworth, UK.
- Ascott, M.J., Marchant, B.P., Macdonald, D., McKenzie, A.A., Bloomfield, J.P., 2017. Improved understanding of spatio-temporal controls on regional scale groundwater flooding using hydrograph analysis and impulse response functions. *Hydrological Processes*, 31(25): 4586-4599. DOI:10.1002/hyp.11380
- Ascott, M.J., McKenzie, A.A., 2022. Analysis of groundwater temperature data in England British Geological Survey, Keyworth, UK.
- Bloomfield, J., Marchant, B., Bricker, S., Morgan, R., 2015. Regional analysis of groundwater droughts using hydrograph classification. *Hydrology and Earth System Sciences*, 19(10): 4327-4344.
- Bloomfield, J.P., Williams, R.J., Goody, D.C., Cape, J.N., Guha, P., 2006. Impacts of climate change on the fate and behaviour of pesticides in surface and groundwater—a UK perspective. *Sci. Total Environ.*, 369(1): 163-177. DOI:<https://doi.org/10.1016/j.scitotenv.2006.05.019>
- Bowes, M.J., Armstrong, L.K., Harman, S.A., Nicholls, D.J.E., Wickham, H.D., Scarlett, P.M., Juergens, M.D., 2020. Weekly water quality data from the River Thames and its major tributaries (2009-2017). NERC Environmental Information Data Centre.
- Burt, S., Burt, T., 2019. Oxford weather and climate since 1767. Oxford University Press.
- Cavelan, A., Golfier, F., Colombano, S., Davarzani, H., Deparis, J., Faure, P., 2022. A critical review of the influence of groundwater level fluctuations and temperature on LNAPL contaminations in the

- context of climate change. *Sci. Total Environ.*, 806: 150412.  
DOI:<https://doi.org/10.1016/j.scitotenv.2021.150412>
- Chen, N., Valdes, D., Marlin, C., Blanchoud, H., Guerin, R., Rouelle, M., Ribstein, P., 2019. Water, nitrate and atrazine transfer through the unsaturated zone of the Chalk aquifer in northern France. *Sci. Total Environ.*, 652: 927-938. DOI:<https://doi.org/10.1016/j.scitotenv.2018.10.286>
- Gervasio, M.P., Soana, E., Granata, T., Colombo, D., Castaldelli, G., 2022. An unexpected negative feedback between climate change and eutrophication: higher temperatures increase denitrification and buffer nitrogen loads in the Po River (Northern Italy). *Environ. Res. Lett.*, 17(8): 084031. DOI:10.1088/1748-9326/ac8497
- Hayashi, M., Rosenberry, D.O., 2002. Effects of Ground Water Exchange on the Hydrology and Ecology of Surface Water. *Groundwater*, 40(3): 309-316. DOI:<https://doi.org/10.1111/j.1745-6584.2002.tb02659.x>
- Hollis, D., McCarthy, M., Kendon, M., Legg, T., Simpson, I., 2019. HadUK-Grid—A new UK dataset of gridded climate observations. *Geoscience Data Journal*, 6(2): 151-159. DOI:10.1002/gdj3.78
- Jones, H., Robins, N., 1999. The Chalk aquifer of the South Downs. British Geological Survey.
- Kendon, M., McCarthy, M., Jevrejeva, S., 2015. State of the UK Climate 2014, Met Office, Exeter, UK.
- Kendon, M., McCarthy, M., Jevrejeva, S., Matthews, A., Sparks, T., Garforth, J., Kennedy, J., 2022. State of the UK Climate 2021. *International Journal of Climatology*, 42(S1): 1-80.  
DOI:<https://doi.org/10.1002/joc.7787>
- Macdonald, D., Dixon, A., Newell, A., Hallaways, A., 2012. Groundwater flooding within an urbanised flood plain. *Journal of Flood Risk Management*, 5(1): 68-80. DOI:<https://doi.org/10.1111/j.1753-318X.2011.01127.x>
- Marchant, B.P., Bloomfield, J.P., 2018. Spatio-temporal modelling of the status of groundwater droughts. *J. Hydrol.*, 564: 397-413. DOI:<https://doi.org/10.1016/j.jhydrol.2018.07.009>
- Marston, C., Rowland, C.S., O'Neil, A.W., Morton, R.D., 2022. Land Cover Map 2021 (10m classified pixels, GB). NERC EDS Environmental Information Data Centre.
- Maurice, L., Bloomfield, J., 2012. Stygobitic Invertebrates in Groundwater — A Review from a Hydrogeological Perspective. *Freshwater Reviews*, 5(1): 51-71, 21.
- McDonough, L.K., Santos, I.R., Andersen, M.S., O'Carroll, D.M., Rutledge, H., Meredith, K., Oudone, P., Bridgeman, J., Goody, D.C., Sorensen, J.P.R., Lapworth, D.J., MacDonald, A.M., Ward, J., Baker, A., 2020. Changes in global groundwater organic carbon driven by climate change and urbanization. *Nat. Commun.*, 11(1): 1279. DOI:10.1038/s41467-020-14946-1
- McKee, T.B., Doesken, N.J., Kleist, J., 1993. The relationship of drought frequency and duration to time scales, *Proceedings of the 8th Conference on Applied Climatology*. American Meteorological Society Boston, MA, pp. 179-183.
- Met Office, 2018. UK Climate Projections. <https://www.metoffice.gov.uk/research/collaboration/ukcp>
- Morton, R.D., Rowland, C.S., Wood, C.M., Meek, L., Marston, C.G., Smith, G.M., 2014. Land Cover Map 2007 (25m raster, GB) v1.2. NERC Environmental Information Data Centre.
- NOAA, 2022. Global Surface Summary of the Day.  
<https://www.ncei.noaa.gov/access/metadata/landing-page/bin/iso?id=gov.noaa.ncdc:C00516>
- Prudhomme, C., Hannaford, J., Harrigan, S., Boorman, D., Knight, J., Bell, V., Jackson, C., Svensson, C., Parry, S., Bachiller-Jareno, N., Davies, H., Davis, R., Mackay, J., McKenzie, A., Rudd, A., Smith, K., Bloomfield, J., Ward, R., Jenkins, A., 2017. Hydrological Outlook UK: an operational streamflow and groundwater level forecasting system at monthly to seasonal time scales. *Hydrological Sciences Journal*, 62(16): 2753-2768. DOI:10.1080/02626667.2017.1395032
- Riedel, T., 2019. Temperature-associated changes in groundwater quality. *J. Hydrol.*, 572: 206-212. DOI:<https://doi.org/10.1016/j.jhydrol.2019.02.059>
- Rivett, M.O., Buss, S.R., Morgan, P., Smith, J.W., Bemment, C.D., 2008. Nitrate attenuation in groundwater: a review of biogeochemical controlling processes. *Water Res.*, 42(16): 4215-4232.
- Sorensen, J.P.R., Butcher, A.S., Stuart, M.E., Townsend, B.R., 2015. Nitrate fluctuations at the water table: implications for recharge processes and solute transport in the Chalk aquifer. *Hydrol. Processes*, 29(15): 3355-3367. DOI:<https://doi.org/10.1002/hyp.10447>
- Stuart, M., Chilton, P., Kinniburgh, D., Cooper, D., 2007. Screening for long-term trends in groundwater nitrate monitoring data. *Quarterly Journal of Engineering Geology and Hydrogeology*, 40(4): 361-376.

- Stuart, M., Chilton, P.J., Butcher, A.S., 2009. Nitrate fluctuations in groundwater: review of potential mechanisms and application to case studies, British Geological Survey, Nottingham, UK.
- Taylor, C.A., Stefan, H.G., 2009. Shallow groundwater temperature response to climate change and urbanization. *J. Hydrol.*, 375(3): 601-612. DOI:<https://doi.org/10.1016/j.jhydrol.2009.07.009>
- Veraart, A.J., de Klein, J.J.M., Scheffer, M., 2011. Warming Can Boost Denitrification Disproportionately Due to Altered Oxygen Dynamics. *PLOS ONE*, 6(3): e18508. DOI:10.1371/journal.pone.0018508
- Webster, R., Oliver, M.A., 1990. *Statistical methods in soil and land resource survey*. Oxford University Press (OUP).
- World Meteorological Organization, 2017. *WMO Guidelines on the Calculation of Climate Normals*, Geneva, Switzerland.
- Worrall, F., Howden, N.J.K., Burt, T.P., Hannah, D.M., 2022. River water temperature demonstrates resistance to long-term air temperature change. *Hydrol. Processes*, 36(11): e14732. DOI:<https://doi.org/10.1002/hyp.14732>
- Zhu, K., Bayer, P., Grathwohl, P., Blum, P., 2015. Groundwater temperature evolution in the subsurface urban heat island of Cologne, Germany. *Hydrol. Processes*, 29(6): 965-978. DOI:<https://doi.org/10.1002/hyp.10209>